Structure−Function Relationships in *Anabaena* Ferredoxin: Correlations between X-ray Crystal Structures, Reduction Potentials, and Rate Constants of Electron Transfer to Ferredoxin:NADP$^+$ Reductase for Site-Specific Ferredoxin Mutants[†,‡]

John K. Hurley,[§] Anne M. Weber-Main,[||] Marian T. Stankovich,[||] Matthew M. Benning,[⊥,#] James B. Thoden,[⊥,#] Janeen L. Vanhooke,[⊥,#] Hazel M. Holden,[⊥,#] Young Kee Chae,[#] Bin Xia,[#] Hong Cheng,[#] John L. Markley,[#] Marta Martinez-Júlvez,[△] Carlos Gómez-Moreno,[△] James L. Schmeits,[§] and Gordon Tollin*[,§]

Department of Biochemistry, University of Arizona, Tucson, Arizona 85721, Department of Chemistry, University of Minnesota, Minneapolis, Minnesota 55455, Department of Biochemistry and Institute for Enzyme Research, University of Wisconsin, Madison, Wisconsin 53706, and Departamento de Bioquímica y Biología Molecular y Celular, Universidad de Zaragoza, E-50009 Zaragoza, Spain

Received April 18, 1997; Revised Manuscript Received June 2, 1997[⊗]

ABSTRACT: A combination of structural, thermodynamic, and transient kinetic data on wild-type and mutant *Anabaena* vegetative cell ferredoxins has been used to investigate the nature of the protein−protein interactions leading to electron transfer from reduced ferredoxin to oxidized ferredoxin:NADP$^+$ reductase (FNR). We have determined the reduction potentials of wild-type vegetative ferredoxin, heterocyst ferredoxin, and 12 site-specific mutants at seven surface residues of vegetative ferredoxin, as well as the one- and two-electron reduction potentials of FNR, both alone and in complexes with wild-type and three mutant ferredoxins. X-ray crystallographic structure determinations have been carried out for six of the ferredoxin mutants. None of the mutants showed significant structural changes in the immediate vicinity of the [2Fe-2S] cluster, despite large decreases in electron-transfer reactivity (for E94K and S47A) and sizable increases in reduction potential (80 mV for E94K and 47 mV for S47A). Furthermore, the relatively small changes in C$^\alpha$ backbone atom positions which were observed in these mutants do not correlate with the kinetic and thermodynamic properties. In sharp contrast to the S47A mutant, S47T retains electron-transfer activity, and its reduction potential is 100 mV more negative than that of the S47A mutant, implicating the importance of the hydrogen bond which exists between the side chain hydroxyl group of S47 and the side chain carboxyl oxygen of E94. Other ferredoxin mutations that alter both reduction potential and electron-transfer reactivity are E94Q, F65A, and F65I, whereas D62K, D68K, Q70K, E94D, and F65Y have reduction potentials and electron-transfer reactivity that are similar to those of wild-type ferredoxin. In electrostatic complexes with recombinant FNR, three of the kinetically impaired ferredoxin mutants, as did wild-type ferredoxin, induced large (approximately 40 mV) positive shifts in the reduction potential of the flavoprotein, thereby making electron transfer thermodynamically feasible. On the basis of these observations, we conclude that nonconservative mutations of three critical residues (S47, F65, and E94) on the surface of ferredoxin have large *parallel* effects on both the reduction potential and the electron-transfer reactivity of the [2Fe-2S] cluster and that the reduction potential changes are not the principal factor governing electron-transfer reactivity. Rather, the kinetic properties are most likely controlled by the specific orientations of the proteins within the transient electron-transfer complex.

Mechanisms of protein-mediated electron-transfer (et)[1] reactions have been under investigation for many years [cf., for example, Tollin (1995), Curry et al. (1995), Durham et al. (1995), Mauk et al. (1995), Millet et al. (1995), Canters and Dennison (1995), Moser et al. (1995, 1992), Tollin et al. (1993), Winkler and Gray (1992), McLendon and Hake (1992); Kostic (1991), and Tollin and Hazzard (1991)], largely as a consequence of their fundamental roles in a wide variety of biological systems. Factors known to be involved in controlling the et process include thermodynamic driving force, distance and relative orientation of redox centers, and

[†] This work has been supported by grants from the National Institutes of Health (DK15057 to G.T., GM29344 to M.T.S., GM30982 to H.M.H., and GM35976 to J.L.M.) and from CICYT (BIO94-0621-CO2-01 to C.G.-M.).

[‡] Coordinates for X-ray crystal structures of the proteins described herein have been deposited in the Protein Data Bank at Brookhaven National Laboratories, Upton, NY (protein and PDB ID code: D62K, 1QOB; D68K, 1QOC; E94K, 1QOD; E95K, 1QOE; Q70K, 1QOF; S47A, 1QOG).

* To whom to address inquiries (E-mail, tollin@biosci.arizona.edu; FAX, (520) 621-9288).

[§] University of Arizona.

[||] University of Minnesota.

[⊥] Institute for Enzyme Research, University of Wisconsin.

[#] Department of Biochemistry, University of Wisconsin.

[△] Universidad de Zaragoza.

[⊗] Abstract published in *Advance ACS Abstracts,* August 15, 1997.

[1] Abbreviations: *Av*FdI, ferredoxin I from *Azotobacter vinelandii*; D68K, aspartic acid at position 68 replaced by lysine (other mutants represented in similar fashion); dRf, 5-deazariboflavin; dRfH$^\bullet$, 5-deazariboflavin semiquinone radical; E_3, CDP-6-deoxy-L-*threo*-D-*glycero*-4-hexulose-3-dehydrase reductase; EDTA, ethylenediaminetetraacetic acid; et, electron transfer; Fd, ferredoxin; Fd_{ox}, oxidized ferredoxin; Fd_{red}, reduced ferredoxin; FNR, ferredoxin:NADP$^+$ reductase; FNR_{red}, hydroquinone form of ferredoxin:NADP$^+$ reductase; FNR_{ox}, oxidized ferredoxin:NADP$^+$ reductase; FNR_{sq}, semiquinone form of ferredoxin:NADP$^+$ reductase; fwhm, full width at half-maximum; HFd, heterocyst cell Fd; MCAD, medium-chain acyl-CoA dehydrogenase; PDR, phthalate dioxygenase reductase; rFNR, recombinant FNR; SCAD, short-chain acyl-CoA dehydrogenase; VFd, vegetative cell Fd; wt, wild type; μ, ionic strength.

S0006-2960(97)00900-8 CCC: $14.00

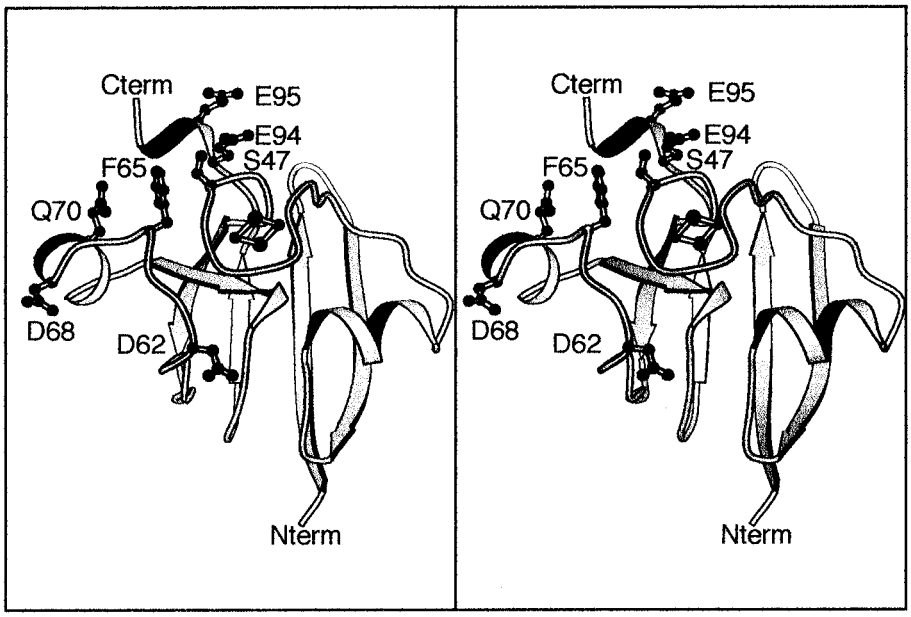

FIGURE 1: Stereoview ribbon diagram of VFd showing pertinent residues. The [2Fe-2S] cluster is not labeled. This figure was generated using the program MOLSCRIPT (Kraulis, 1991).

composition of the intervening protein matrix, including the interface between protein molecules within an intermediate complex.

Previous investigations from these laboratories have focused on the et reaction between ferredoxin (Fd) and ferredoxin:$NADP^+$ reductase (FNR) from the cyanobacterium *Anabaena* as a model for interprotein redox interactions [for a review of earlier structure−function studies on these proteins, see Holden et al. (1994)]. Although Fd is involved in a variety of metabolic pathways (Knaff & Hirasawa, 1991; Lovenberg, 1973, 1974, 1977), its interaction with FNR occurs within the plant and cyanobacterial photosynthetic et chains, where it functions as the terminal electron acceptor from photosystem I, transferring electrons to FNR which mediates the two-electron reduction of $NADP^+$ to NADPH:

$$2Fd_{red} + NADP^+ + H^+ \xrightarrow{FNR} 2Fd_{ox} + NADPH \quad (1)$$

The individual wild-type (wt) proteins in the *Anabaena* Fd/FNR system have been well characterized. Wt Fd from vegetative cells of *Anabaena* 7120 (hereafter referred to as VFd) has been cloned and overexpressed in *Escherichia coli* (Alam et al., 1986), and its three-dimensional structure has been solved to high resolution (Holden et al., 1994; Rypniewski et al., 1991), thereby making it a good candidate for structure−function studies using site-directed mutagenesis. This "plant-type" Fd contains a [2Fe-2S] prosthetic group in an 11 kDa polypeptide chain. Its reduction potential has been reported to be in the range of −406 to −440 mV by various procedures (Vidakovic et al., 1995; Hurley et al., 1993a; Böhme & Schrautemeier, 1987a). An X-ray crystal structure has also been solved (Jacobson et al., 1992, 1993) for the heterocyst cell Fd from *Anabaena* (hereafter referred to as HFd). This isozyme of VFd can receive electrons from NADPH via FNR and then transfer these electrons to the Fe protein of nitrogenase in specialized N_2-fixing cells (Böhme & Haselkorn, 1988; Böhme & Schrautemeier, 1987a,b). Thus, the electron flow is in the reverse direction compared to photosystem I. The amino acid sequence of HFd is 51% identical to the vegetative form, and its reduction potential has been reported to be 28 mV less negative than VFd (Böhme & Schrautemeier, 1987a).

FNR isolated from *Anabaena* 7119 is a 36 kDa protein containing one noncovalently bound FAD as its prosthetic group. It also has been cloned and overexpressed in *E. coli* (Fillat et al., 1990, 1994), and its three-dimensional structure has been determined (Serre et al., 1996). FNR can accept a pair of electrons in two one-electron steps involving an intermediate FAD semiquinone. The midpoint two-electron reduction potential (E_m) has been reported to be in the range of −320 to −344 mV (Pueyo et al., 1991; Sancho et al., 1988). The one-electron potential of the oxidized/semiquinone couple ($E_1°'$) has been calculated to be −370 mV (Sancho et al., 1988).

For the VFd/FNR interaction, previous kinetic results (Hurley et al., 1993a; Walker et al., 1991) are consistent with a minimal two-step mechanism involving intermediate complex formation followed by et, as depicted in eq 2. We

$$VFd_{red} + FNR_{ox} \overset{K_d}{\rightleftharpoons} (VFd_{red}{:}FNR_{ox}) \xrightarrow{k_{et}} VFd_{ox} + FNR_{red} \quad (2)$$

have probed this mechanism using site-directed mutagenesis, coupled with laser flash photolysis transient absorbance measurements (Tollin, 1995; Tollin et al., 1993; Tollin & Hazzard, 1991) which follow the kinetics of et from reduced VFd to oxidized FNR. In evaluating the effects of a wide range of mutations on this protein−protein interaction, we have previously identified two residues in VFd (F65 and E94; see Figure 1) as being crucial to the et reaction with FNR (Hurley et al., 1993a). We have shown that the residue at position 65 must be aromatic (Hurley et al., 1993b) and the residue at position 94 must be acidic (Hurley et al., 1994), in order to obtain efficient et. For both residues, the K_d values for the binding of oxidized nonconservative VFd mutants to oxidized FNR were not appreciably altered, and thus it was concluded that diminished complex stability was not the cause of et inactivity (Hurley et al., 1993a). In addition, analogous nonconservative mutations at nearby residues (e.g., E95K) produced proteins which retained wt

Table 1: Second-Order Rate Constants for Oxidation of Reduced VFd by Oxidized FNR[a] and Reduction Potentials of Mutant and Wt VFd and HFd

Fd	$k \times 10^{-8}$ (M^{-1} s^{-1})	$E^{\circ\prime}$ (mV)[e]	Fd	$k \times 10^{-8}$ (M^{-1} s^{-1})	$E^{\circ\prime}$ (mV)[e]
wt[b]	1.2 ± 0.1	−384	E94Q[d]	<0.0001	−319
HFd[b]	1.8 ± 0.2	−351	E95K[b,f]	1.2 ± 0.1	−372
D62K[f]	1.0 ± 0.1	−373	F65A[b]	<0.0001	−291
D68K[b,f]	1.9 ± 0.2	−380	F65I[b]	<0.0001	−328
Q70K[f]	1.0 ± 0.6	−382	F65Y[c]	1.3 ± 0.2	−390
E94D[d]	1.3 ± 0.5	−367	S47A[f]	<0.005	−337
E94K[b,f]	<0.0001	−304	S47T	0.9 ± 0.1	−438

[a] Rate constants were measured at an ionic strength of 12 mM. For the determination of second-order rate constants, typically five to six protein concentrations over the range of 5−40 μM were used. In the case of the oxidation of reduced VFd by FNR, aliquots of a solution of oxidized FNR were added to a sample containing 30 or 40 μM Fd. [b] Taken from Hurley et al. (1993a). [c] Taken from Hurley et al. (1993b). [d] Taken from Hurley et al. (1994). [e] Measurements were performed as described in Materials and Methods in 50 mM potassium phosphate buffer and 1 mM EDTA, pH 7.5, 4 °C, at approximately 100 mM ionic strength (the potential of wt Fd measured at 12 mM ionic strength was very similar to the value at 100 mM; data not shown). Experimental error ranged from ±1 to 3 mV for all Fds examined. [f] X-ray crystal structures are presented for these mutant ferredoxins (see text).

et reactivity (Hurley et al., 1993a). On the basis of these results, it was concluded that very specific protein−protein interactions at the VFd/FNR interface control the mutual orientation of the proteins within an intermediate complex, allowing the formation of a productive complex which supports efficient et (Hurley et al., 1993a). More recent experiments have demonstrated the importance of hydrophobic interactions between VFd and FNR in forming a productive et complex (Hurley et al., 1996a) and have indicated that electrostatic interactions favor less productive orientations between the two proteins, resulting in a decrease in the rate constant for et at ionic strengths below about 100 mM.

In the present work, we sought to further test the hypothesis that the formation of a productive et complex between VFd and FNR is tightly controlled by specific protein−protein interactions at the docking interface of the two proteins. In order to do this, we have compared kinetic results with X-ray crystallographic structures and thermodynamic properties (i.e., reduction potentials) for a variety of VFd mutants. Clearly, significant changes in either the three-dimensional structure and/or the reduction potential of a mutant VFd could result in kinetic inactivity with FNR. Large protein structural changes could either prohibit binding altogether or else result in a stable, but nonproductive complex (perhaps by altering the pathway of et). Alternatively, shifts in reduction potential of either the [2Fe-2S] center of the mutant VFd, the FAD center of VFd-bound FNR, or both redox centers could produce a thermodynamic barrier to et. In the latter context, site-directed mutagenesis of residues in the iron−sulfur cluster binding loop of VFd from *Anabaena* 7120 has been shown to perturb the [2Fe-2S] reduction potential (Vidakovic et al., 1995; Cheng et al., 1994; Weber-Main et al., in preparation; Hurley et al., in preparation). In the present experiments, we have focused on VFd mutations in surface residues in the vicinity of the cluster (see Table 1). Cross-linking (Vieira et al., 1986; Zanetti et al., 1988), chemical modification (Vieira et al., 1986), and computer modeling studies (Karplus, 1991; Karplus et al., 1991; De Pascalis et al., 1993) have implicated some of these residues in interactions with FNR. Thus, charge-reversal mutations were made at acidic residues (D62, D68, Q70K, E94, E95) likely to interact electrostatically with basic residues of FNR. Characterizations of the D68K (Hurley et al., 1996b), E95K (Hurley et al., 1993a), and E94K (Hurley et al., 1993a, 1994) mutants have been reported previously. All of the mutated residues (including F65) are highly conserved among plant-type Fds from cyanobacteria, algae, and higher plants, and some play an important structural role in binding the [2Fe-2S] cluster to the protein backbone (i.e., E94, S47; Holden et al., 1994). We were especially interested in examining the kinetically "dead" VFd mutants at positions E94 and F65 (those mutants having et reactivities toward FNR, as determined by transient kinetic measurements, which are two or more orders of magnitude lower than wt VFd, are referred to as dead mutants in the present communication) to determine if acidity and aromaticity play a role in modulating their reduction potentials as well as their et kinetics. Furthermore, during the course of these investigations, transient kinetics were obtained for several new mutants of VFd, including two at an additional residue (S47) which has now been found to also be critical to the et reaction with FNR. X-ray crystal structures were successfully solved for six VFd mutants, and reduction potentials were determined for VFd, HFd, and 12 VFd mutants, both alone and in complex with recombinant *Anabaena* 7119 FNR (rFNR). It will be shown below that those amino acid residues found to be critical for the protein−protein et process also play a disproportionately large role in determining the intrinsic reduction potential of the [2Fe-2S] center of VFd. Taken together, the data support the contention that the principal determinant of et reactivity in this group of ferredoxins is the mutual orientation of the reaction partners within the transient protein−protein complex, rather than structural perturbations or changes in thermodynamic properties.

MATERIALS AND METHODS

Protein Preparation and Mutagenesis. Wt and mutant (except for those at position 65) VFds from *Anabaena* strain 7120 were prepared at the University of Arizona by previously described methods (Hurley et al., 1993a); Vfd mutants at position 65 were generated at the University of Wisconsin [cf. Cheng et al. (1994) for methodology]. HFd was prepared at the University of Wisconsin according to Jacobson et al. (1992). Native FNR was isolated and purified as described by Pueyo and Gomez-Moreno (1991). The 36 kDa form of recombinant FNR was prepared by the method of Fillat et al. (1994).

Optical Methods and Binding Constant Measurements. Protein extinction coefficients and methods used to obtain absorption spectra and circular dichroism spectra have been reported earlier (Hurley et al., 1993a). The UV/visible and CD spectra of all VFd mutants were essentially indistinguishable from those of the wt protein. This indicates that no significant changes in cofactor environment occurred as a consequence of mutagenesis. Binding constants for the transient $VFd_{red}-FNR_{ox}$ complex were obtained by fitting kinetic data to the exact solution of the differential equation describing the (minimal) two-step mechanism (see eq 2 above; Simondsen & Tollin, 1983; Simondsen et al., 1982).

Laser Flash Photolysis for Transient Kinetic Measurements. The laser flash photolysis system, including associated optical and electronics systems, used to monitor the reaction kinetics has been described (Hurley et al., 1996b;

Przysiecki et al., 1985; Bhattacharyya et al., 1983; in the current laser system the Nicolet 1170 signal averager has been replaced by a Tektronix TDS410A digitizing oscilloscope). The photochemical reaction by which the 5-deazariboflavin (dRf) triplet state initiates protein−protein et has also been described (Tollin, 1995; Tollin et al., 1993; Tollin & Hazzard, 1991). All kinetic experiments were performed at room temperature, under pseudo-first-order conditions in which VFd is present in large excess over the dRfH$^{\bullet}$ generated by the laser flash (<1 μM) [see Walker et al. (1991) for additional details]. Under these conditions, dRfH$^{\bullet}$ reacts almost exclusively with oxidized VFd when both VFd and smaller amounts of FNR are present simultaneously (Walker et al., 1991). This allows the one-electron transfer from reduced VFd to oxidized FNR to be monitored. All of the kinetic experiments described below were carried out using native FNR.

Solutions of dRf (95−100 μM in 4 mM phosphate buffer, pH 7.0, containing 1 mM EDTA) were made anaerobic by bubbling for 1 h with H_2O-saturated argon. Microliter volumes of concentrated protein solutions were introduced into this solution in a 1 cm cuvette through a rubber septum, and Ar gas was blown over the sample surface to remove any added oxygen. Generally, data from four to eight laser flashes were averaged. Ionic strength was adjusted by adding small aliquots of 5 M NaCl. Digitized kinetic traces were analyzed using a computer fitting routine (Kinfit, OLIS Co., Bogart, GA).

Spectroelectrochemistry for Reduction Potential Measurements. All of the electrochemical experiments described below were performed using recombinant FNR. Dithionite titrations of wt Fds and rFNR were carried out to confirm the number of reducing equivalents necessary to fully reduce each protein. All experiments were conducted at pH 7.5 and 4 °C in 50 mM potassium phosphate buffer. Typically, a 25 μM protein solution was reduced with a degassed sodium dithionite solution (buffered at pH 8.5 in a 20 mM sodium pyrophosphate buffer) which was standardized with lumiflavin 3-acetate (generously provided by Dr. Sandro Ghisla, University of Konstanz, Germany). Protein solutions were sealed in a glass spectroelectrochemical cell (Stankovich, 1980) and made anaerobic by continuous cycles of argon and vacuum over a period of 1−2 h. Deoxygenated sodium dithionite was added through one of the cell ports with an air-tight 500 μL Hamilton syringe. A spectrum was recorded after each addition with a Perkin-Elmer 2S or 12S UV/visible spectrophotometer interfaced with an IBM-compatible computer.

Potentiometric titrations of wt VFd, mutant VFds, HFd, and rFNR were performed using a three-electrode spectroelectrochemical cell previously described (Stankovich, 1980; Stankovich & Fox, 1983). Typical experimental solutions contained 20−50 μM protein, 1−5 μM indicator dyes, 1 μM 5-deazaflavin, and 1 mM EDTA in 50 mM potassium phosphate buffer at pH 7.5 and 4 °C. Indicator dyes were selected to cover the experimental potential range of each protein titration. These included lumiflavin 3-acetate, −221 mV at pH 7.5; benzyl viologen (Sigma), −354 mV; and methyl viologen (Sigma), −443 mV. All potentials in this study are reported versus the standard hydrogen electrode. The 5-deazaflavin (gift of Dr. Sandro Ghisla) and EDTA were present to initiate photoreduction of proteins via the strongly reducing deazaflavin radical (Massey & Hemmerich, 1978). Alternative reduction methods—sodium dithionite (VFd and rFNR experiments) or electrochemical mediation by methyl viologen (rFNR experiments)—yielded similar results. Experimental solutions were made anaerobic through several cycles of argon and vacuum over a total period of 2 h. Stepwise photoreduction of proteins was achieved by irradiating the solution (with the cell immersed in ice water) with a 650 W projector bulb for 5−30 s per titration point. After reduction, the cell was placed in a temperature-controlled holder in a Perkin-Elmer 2S or 12S UV/visible spectrophotometer interfaced with an IBM-compatible computer. Protein potentials were measured with an Orion Research Model 601A digital ion analyzer. Equilibration of the system was considered established when the measured potential remained stable within 1−2 mV for 10 min, typically taking 30 min per titration point. A UV/visible spectrum was then collected. Spectra were later corrected for turbidity and dye contributions using the Perkin-Elmer PECSS spectral subtraction program.

For VFd titrations, concentrations of the oxidized (VFd_{ox}) and one-electron reduced (VFd_{red}) protein at each point were determined from Beer's law and the absorbance at 463 nm. The extinction coefficients of VFd_{ox} and HFd_{ox} ($\epsilon_{463} = 9150$ M^{-1} cm^{-1} and $\epsilon_{466} = 9000$ M^{-1} cm^{-1}, respectively) were determined by using amino acid analysis to determine the concentration of a protein solution whose UV/visible spectrum had been recorded previously. Values obtained in this manner agreed well with those previously reported in the literature (Böhme & Haselkorn, 1989). The extinction coefficients of Fd_{red} ($\epsilon_{463} = 3700$ M^{-1} cm^{-1} for VFd_{red} and $\epsilon_{466} = 3900$ M^{-1} cm^{-1} for HFd_{red}) were derived from spectral titrations in this study. Extinction coefficients at 463 nm for all VFd mutants were assumed to be identical to those of wt VFd.

With the concentrations of each redox species and measured equilibrium potentials (E) in hand, the formal one-electron reduction potential ($E^{\circ\prime}$) of the [2Fe-2S] cluster in each VFd and the number of electrons transferred in the reaction (n) were calculated by a computerized nonlinear regression fit (Duggleby, 1981) to the Nernst equation.

For rFNR titrations, concentrations of the oxidized ($rFNR_{ox}$), one-electron reduced semiquinone ($rFNR_{sq}$), and two-electron fully reduced ($rFNR_{red}$) species at each point were calculated by simultaneously solving three equations: a mass balance equation and two Beer's law relationships for 458 and 600 nm. Extinction coefficients used for redox species quantitation at 458 and 600 nm were 9400 M^{-1} cm^{-1} (Pueyo & Gomez-Moreno, 1991) and 200 M^{-1} cm^{-1} (calculated from spectral titrations), respectively, for $rFNR_{ox}$; 3400 and 4000 M^{-1} cm^{-1} (spinach FNR_{sq} values; Batie & Kamin, 1984), respectively, for $rFNR_{sq}$; and 900 M^{-1} cm^{-1} (Pueyo & Gomez-Moreno, 1991) and 300 M^{-1} cm^{-1} (calculated from spectral titrations), respectively, for $rFNR_{red}$. The Nernst equation was used in calculating the two-electron midpoint potential (E_m) and individual formal potentials for each one-electron step ($E_1^{\circ\prime}$ for $FNR_{ox/sq}$ and $E_2^{\circ\prime}$ for the $FNR_{sq/red}$ couple). The maximal amount of semiquinone stabilized thermodynamically (M) was calculated according to eq 3 (Clark, 1960). For all potentiometric titrations,

$$E_1^{\circ\prime} - E_2^{\circ\prime} + 0.11 \log[2M/(1 - M)] \qquad (3)$$

the typical error in reduction potential measurements was ±1−3 mV.

Potentiometric titrations of VFd−rFNR complexes were conducted, as described above for the single protein experi-

ments, on 1:1 mixtures of VFd and rFNR (approximately 15−40 μM each protein) in 4 mM potassium phosphate buffer and 1 mM EDTA, pH 7.5, 4 °C, at an ionic strength of 12 mM. Complex formation is complete under these conditions. Extinction coefficients for the complexed proteins were assumed to be identical to those of their uncomplexed values. Concentrations of the five redox species present at each point in the titration (VFd_{ox}, VFd_{red}, $rFNR_{ox}$, $rFNR_{sq}$, and $rFNR_{red}$) were determined from the solution of five simultaneous equations: two mass balance equations and three Beer's law relationships at 485, 458, and 422 nm.

Crystallization, X-ray Data Collection, and Least Squares Refinement. X-ray diffraction quality crystals of the six site-directed mutant VFds reported here were grown at 4 °C by the hanging drop method of vapor diffusion as previously described (Rypniewski et al., 1991). The precipitant solution typically contained 2.6 M ammonium sulfate, 50 mM potassium succinate (pH 5.5), and 1% 2-methyl-2,6-pentanediol. Three of the mutants, namely D62K, Q70K, and S47A, crystallized in the space group $P2_12_12_1$ with unit cell dimensions of $a = 37.6$ Å, $b = 38.1$ Å, and $c = 147.4$ Å and two molecules per asymmetric unit. The other three mutants, E94K, E95K, and D68K, crystallized in the space group $P3_221$ with unit cell dimensions of $a = b = 38.3$ Å and $c = 136.2$ Å and one molecule in the asymmetric unit.

Complete X-ray data sets for the mutant proteins were collected from single crystals at 4 °C with a Siemens X1000D area detector system. The X-ray source was nickel-filtered Cu Kα radiation from a Rigaku RU200 X-ray generator operated at 50 kV and 50 mA. All X-ray data were processed with the data reduction software package XDS (Kabsch, 1988a,b) and internally scaled according to a procedure developed in the laboratory by Dr. Gary Wesenberg. Relevant X-ray data collection statistics are available as Supporting Information.

Since the original structural investigation of the wt Vfd employed the orthorhombic crystal form, the D62K, Q70K, and S47A ferredoxin structures were solved by difference Fourier techniques. For the E94K, E95K, and D68K mutant protein structures, the wt ferredoxin served as the search model for molecular replacement procedures with the program AMORE (Navaza, 1987).

All of the models reported here were subjected to alternate cycles of least squares refinement with the program TNT (Tronrud et al., 1987) and manual-model building with the software package FRODO (Jones, 1985). During the refinements, the geometries of the [2Fe-2S] clusters were restrained to that observed in the small-molecule structural determination of $(Et_4N)_2[FeS(SCH_2)_2C_6H_4]_2$ by Mayerle et al. (1973). Relevant refinement statistics are available as supporting information. Representative electron density maps are shown in panels A and B of Figure 2 for the mutated regions (bottom panels) of the mutants Q70K and S47A, respectively. The upper panels of Figure 2 show the electron density maps corresponding to the wt protein.

RESULTS

Transient Kinetics. When a solution containing EDTA and dRf is subjected to a laser flash, a rapid increase in absorption is observed at 507 nm, corresponding to the formation of the dRf semiquinone radical ($dRfH^{\bullet}$) as a consequence of H atom abstraction from EDTA by the dRf triplet state. If VFd (or a VFd mutant) is also present, there is a subsequent rapid decrease in absorbance at 507 nm due to the reaction of VFd with $dRfH^{\bullet}$, resulting in the formation of VFd_{red} (see Figure 3). Wt VFd and all Vfd mutants studied to date have been found to react with $dRfH^{\bullet}$ with very similar second-order rate constants (the average value for the mutants is $1.6 \pm 0.3 \times 10^8$ M^{-1} s^{-1}; that of wt VFd is $2.2 \pm 0.2 \times 10^8$ M^{-1} s^{-1}). We take this as evidence that the accessibility and intrinsic reactivity of the [2Fe-2S] cluster in these mutants have not been appreciably perturbed.

When native FNR is also present in the reaction mixture, one observes a subsequent slower increase in absorbance due to the oxidation of VFd_{red} by FNR_{ox} with concomitant formation of FNR_{sq}. This sequence of absorbance changes is shown in Figure 3 for wt VFd and five representative mutants: D68K, D62K, Q70K, E94K, and S47A. Note that the slow increase in absorbance due to FNR reduction is *not* observed on these time scales for the E94K and S47A mutants. This indicates that these mutants either do not react with FNR or react much more slowly than either VFd or the other mutants. This highly impaired et reactivity has previously been reported for E94K and E94Q mutants (Hurley et al., 1993a, 1994). The result with the S47A mutant is new to the present investigation.

Titrations of varying amounts of native FNR into solutions containing VFd, dRf, and EDTA at low ionic strength (μ = 12 mM) yielded linear pseudo-first-order kinetic plots [data not shown; see Hurley et al. (1993a) for examples]. These allowed the calculation of second-order rate constants which reflect both the dissociation constant for complex formation (K_d) and the limiting et rate constant (k_{et}) for the VFd_{red}/FNR_{ox} interaction (see eq 2 above). These rate constants are shown in Table 1, where it is seen that HFd and the mutants D62K, D68K, Q70K, E94D, E95K, F65Y, and S47T react essentially like wt VFd under these conditions. In sharp contrast, the F65A and F65I mutants [cf. Hurley et al. (1993a,b)], in addition to E94K, E94Q, and S47A, are severely impaired in their ability to transfer electrons to FNR. These dead mutants reacted so slowly that an FNR titration was not possible, and the upper limit for the rate constant given in Table 1 was estimated from a single decay curve taken on a 5 s time scale. It is important to note that, unlike S47A, the S47T mutant showed wt-like reactivity toward FNR. This demonstrates the importance of the hydroxyl group at position 47 in VFd for efficient et.

The ionic strength profiles of HFd and the mutant VFds revealed interesting differences. HFd reacts with FNR with a rate constant that is slightly smaller than VFd at all values of μ, and its ionic strength dependence curve is approximately parallel to that of VFd (Figure 4). This result correlates with the smaller overall negative charge on HFd compared with VFd (−9 for HFd vs −14 mV for VFd). At increasing values of μ, the observed pseudo-first-order rate constants for D62K, Q70K, and S47T were found to decrease much more dramatically than does the rate constant for VFd (see Figure 4). It has previously been shown that E95K (Hurley et al., 1993a) and F65Y (Hurley et al., 1993b) react essentially like VFd at all ionic strengths, whereas E94D (Hurley et al., 1994) reacts like VFd at low values of μ and with a somewhat smaller rate constant at higher values of μ. Earlier studies have also demonstrated that D68K reacts considerably faster than VFd at low values of μ (Hurley et al., 1995a, 1996b) but reacts much like wt at μ values above about 80 mM.

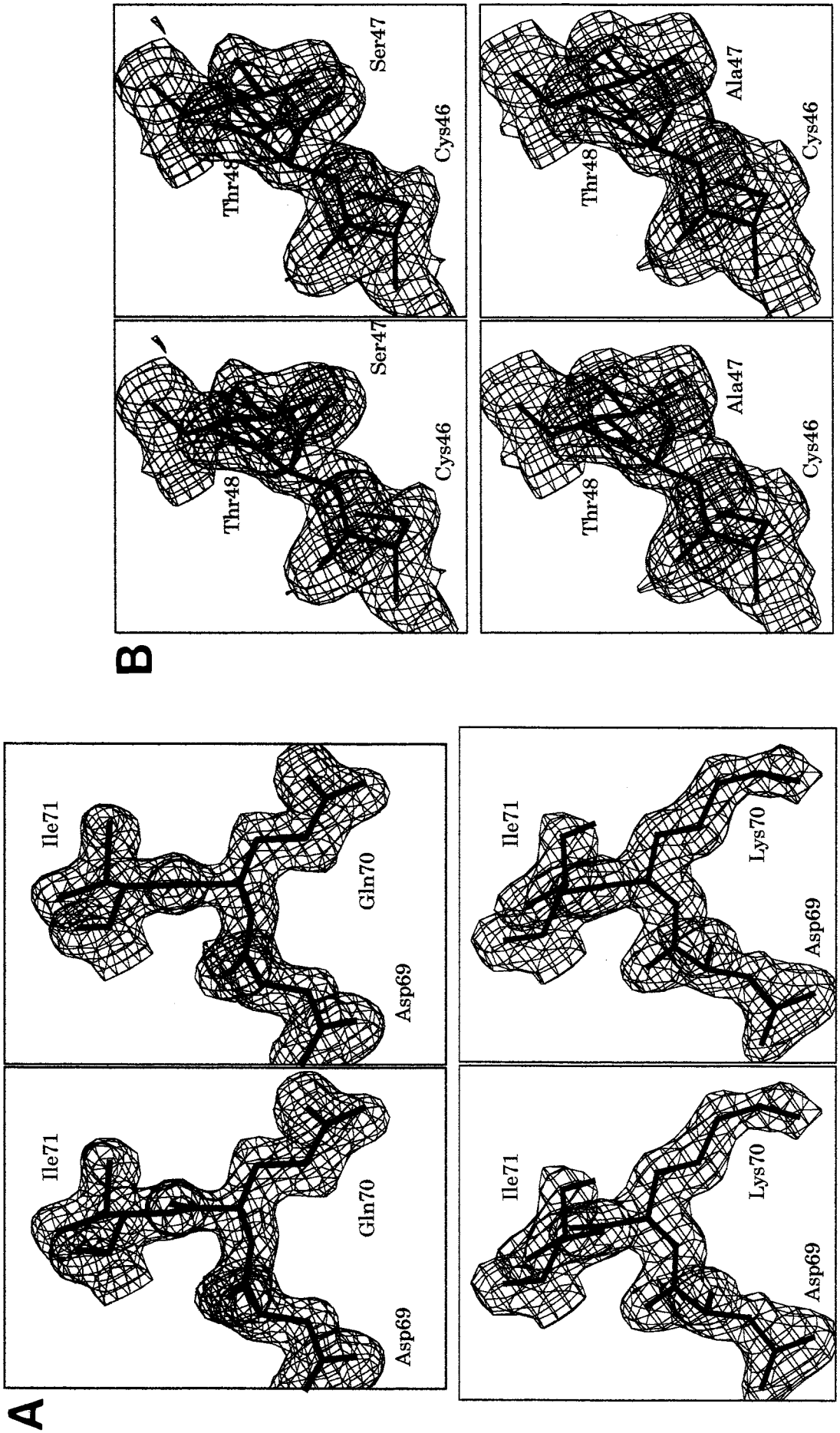

FIGURE 2: Representative electron density maps of the VFd mutants Q70K (A, lower) and S47A (B, lower). Corresponding electron density maps for the wt protein are shown in the upper panels. The electron density shown was calculated to 1.8 Å resolution with coefficients of the form $(2F_o - F_c)$, where F_0 and F_c were the observed and calculated structure factor amplitudes, respectively. The map was contoured at 1σ. The figures were prepared with the software package FROST, written by Dr. Gary Wesenberg, University of Wisconsin.

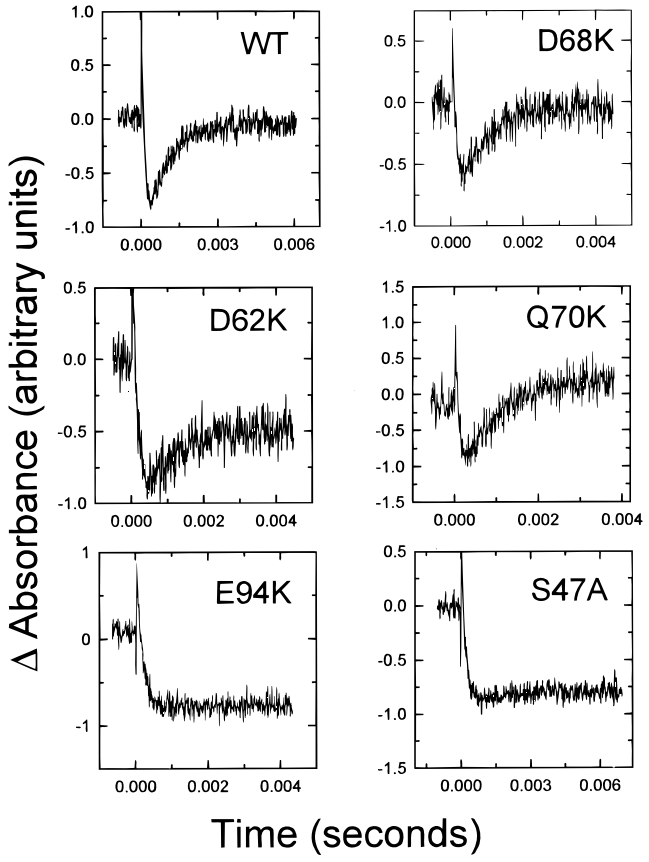

FIGURE 3: Transient decay curves of wt and mutant VFds plus native FNR. Shown are curves for 40 μM wt VFd + 5 μM FNR, 40 μM D68K + 10 μM FNR, 40 μM D62K + 15 μM FNR, 30 μM Q70K + 10 μM FNR, 30 μM E94K + 10 μM FNR, and 30 μM S47A + 5 μM FNR. Solutions also contained 1 mM EDTA and 95−100 μM dRf. The ionic strength was 12 mM. The monitoring wavelength was 507 nm. Wt data are taken from Hurley et al. (1993a).

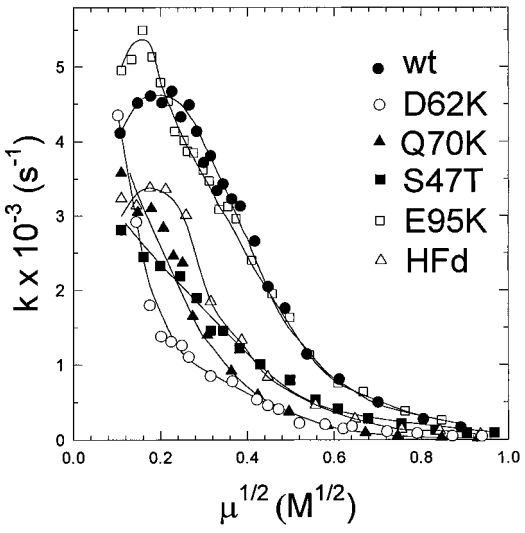

FIGURE 4: Ionic strength dependence of native FNR reduction by mutant and wt VFds. Experiments with wt VFd and HFd were done at 30 μM in each protein. Experiments with the VFd mutants utilized 30 μM FNR and 40 μM mutant Fd. Ionic strength was adjusted using aliquots of 5 M NaCl. Other solution conditions as given in Figure 2. Wt data are taken from Hurley et al. (1993a), and the D68K data are taken from Hurley et al. (1995).

In marked contrast, the observed rate constants for the highly impaired E94K and F65A mutants increase monotonically by only a factor of approximately 8 (0.5−4 s^{-1}) over a 12−750 mM range of μ (Hurley et al., 1993a). Furthermore, the impaired E94Q (Hurley et al., 1994) and F65I mutants (data not shown) reacted similarly to E94K and F65A, with the observed first-order rate constants increasing to only 0.5 and 1.5 s^{-1}, respectively, at the highest values of μ. Due to its marked unreactivity, an ionic strength dependence curve could not be obtained for the S47A mutant. The reason previously proposed for the ionic strength behavior of these dead mutants was that the mutual orientation of the proteins in the intermediate complexes formed between FNR and these mutant VFds was so far from optimal for efficient et that any "loosening" of the complex by addition of salt allowed the attainment of more productive orientations (Hurley et al., 1993a, 1994).

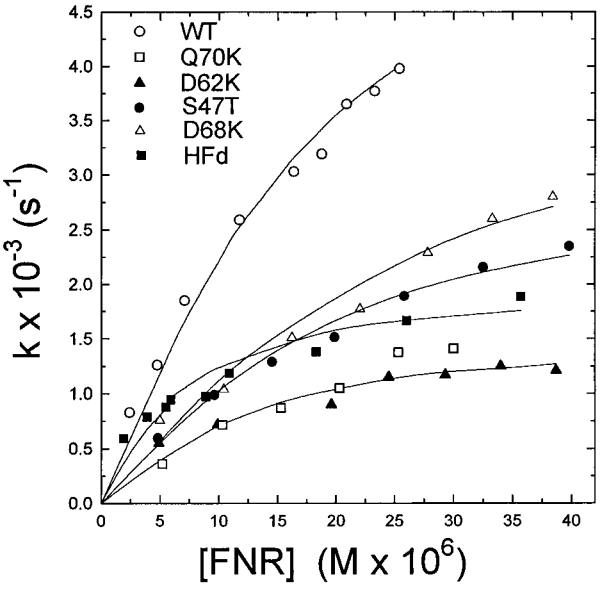

FIGURE 5: Concentration dependence of native FNR reduction by wt and mutant VFds at 100 mM ionic strength. FNR was titrated into solutions containing 30 μM wt or Q70K VFd or into solutions containing 40 μM D62K, S47T, or D68K VFds. Ionic strength was adjusted using 5 M NaCl. Other solution conditions are as in Figure 2. Wt data are taken from Hurley et al. (1996a).

Previous studies (Hurley et al., 1993a, 1996a) showed that k_{obs} for VFd had a hyperbolic dependence on the FNR concentration at $\mu = 100$ mM, as is expected for the reaction mechanism given in eq 2. The difference between this behavior and that observed at low ionic strength has been attributed (Hurley et al., 1996a) to the fact that the preformed VFd−FNR complex, which is present in significant amounts under low μ conditions, cannot be reduced by either dRfH$^{\bullet}$ or VFd_{red}. The expected hyperbolic dependence is obtained after correction for the concentration of complexed FNR; although this correction does not change k_{et}, it decreases the absolute values obtained for K_d, without affecting their relative values. Figure 5 shows plots of k_{obs} versus FNR concentration for wt VFd, HFd, and the mutants Q70K, D62K, S47T, and D68K at 100 mM ionic strength; the corresponding values of K_d (uncorrected) and k_{et} are given in Table 2. As seen from these data, HFd has a k_{et} value which is about 33% that of VFd; since HFd has only 51% sequence homology with VFd, it is difficult to ascribe its lowered reactivity to particular amino acid residues. These data also indicate decreases in k_{et} relative to wt VFd of 30% for D68K, 50% for S47T, and 75% each for Q70K and D62K. While these mutations have clearly affected k_{et}, the degree of the perturbation is several orders of magnitude smaller than for the dead mutants E94Q and F65I (although

Table 2: Kinetic Parameters for Wt and Mutant Fds and for HFd at $\mu = 100$ mM[a]

Fd	K_d[b] (μM)	k_{et} (s^{-1})
wt[c]	9.3 ± 0.7	6200 ± 400
HFd	4.2 ± 0.5	2000 ± 200
D68K	13.6 ± 1.3	4100 ± 400
Q70K	5.5 ± 0.3	1500 ± 100
S47T	10.9 ± 0.5	3100 ± 150
D62K	5.5 ± 0.3	1500 ± 100

[a] These values were obtained from the data in Figure 5 as described in the text. [b] Values not corrected for preformed complex (see text). [c] Taken from Hurley et al. (1996a).

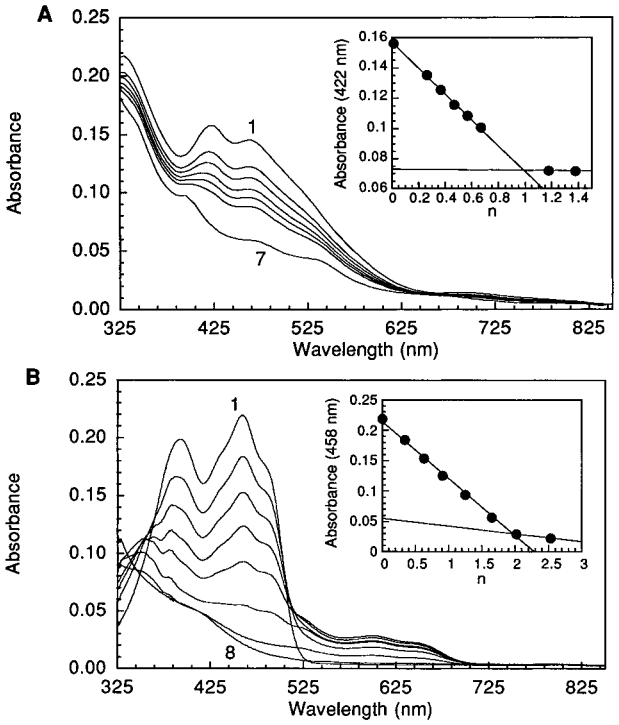

FIGURE 6: Dithionite titrations of wt VFd (A) and rFNR (B) in 50 mM potassium phosphate buffer, pH 7.5 at 4 °C. For VFd, spectrum 1 is fully oxidized, and spectrum 7 is fully reduced. For rFNR, spectrum 1 is fully oxidized, and spectrum 8 is fully reduced. The insets to (A) and (B) show a plot of UV/visible absorbance versus *n*, the number of reducing equivalents added.

we were not able to measure limiting k_{et} values for the F65A and S47A mutants, we presume that these two mutants are similarly dead). At $\mu = 100$ mM, FNR titration data for E94Q and F65I showed that et was rate-limiting over the accessible concentration range, with first-order rate constants of 0.3 s^{-1} (Hurley et al., 1994) and 0.6 s^{-1} (Hurley et al., 1993b), respectively. S47A was so unreactive as to preclude determination of the limiting et rate constant, even at increased concentrations of FNR. It is also evident from Table 2 that the K_d values (for the transient $Fd_{red}-FNR_{ox}$ complex) for those mutants for which we have such data were not greatly affected by the mutations; i.e., all are within a factor of approximately 2 of the wt protein. Furthermore, no apparent correlation exists between complex stability and k_{et}.

Spectral Properties and Reduction Potentials of Free Fds and rFNR. Wt and mutant VFds and rFNR were each titrated with a standardized solution of sodium dithionite to quantitate the number of equivalents required to fully reduce the redox moiety in each protein (Figure 6). These experiments also enabled us to monitor the visible spectral properties of each protein throughout the reduction without spectral interference from indicator dyes. As seen in the insets to Figure 6, addition of the theoretical number of equivalents (1 and 2, respectively) yielded fully reduced VFd and rFNR. Similar results were observed for HFd (data not shown). Assuming a molar absorptivity at 600 nm of 4000 M^{-1} cm^{-1} as for spinach FNR (Batie & Kamin, 1984), approximately 31% blue neutral FNR_{sq} was kinetically stabilized. All VFd mutants exhibited visible spectra nearly identical to that of wt VFd in their oxidized, reduced, and mixed redox state forms generated throughout the titration.

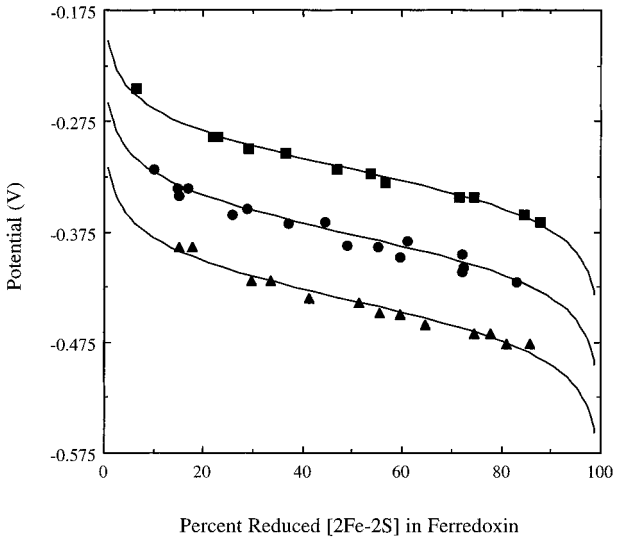

FIGURE 7: Plot of reduction potential versus the percent reduced [2Fe-2S] in *Anabaena* vegetative ferredoxins. Points were collected during spectroelectrochemical titrations as described in Materials and Methods: wt (●); E94Q (■); S47T (▲). The theoretical curves deduced from the spectroelectrochemically determined reduction potentials are plotted as solid lines.

Values for the reduction potentials of wt and mutant *Anabaena* 7120 VFds at pH 7.5 and 4 °C are listed in Table 1. Each VFd displayed Nernstian behavior based on the slopes of their Nernst plots (close to 55 mV, the theoretical slope for a one-electron transfer at the experimental temperature) and their *n* values calculated from the nonlinear fits. Representative titration data are shown for VFd, E94Q, and S47A in Figure 7. All mutants exhibited stability similar to VFd, regenerating >95% oxidized VFd upon reoxidation in air at the end of each titration.

It should be noted that the differences observed between the wt VFd reduction potentials measured in this study and those reported by other investigators (Hurley et al., 1993a; Vidakovic et al., 1995) are in all likelihood due to differences in methodology and experimental conditions. That methodology can influence the measured potential of VFd is apparent from the work of Vidakovic et al. (1995), who reported two different potentials for Vfd which depended on the method used (−406 mV by spectrophotometric redox titration and −439 mV by differential pulse voltammetry). While the absolute reduction potentials determined in this study for VFd and HFd (−384 mV and −351 mV, respectively) differ from those originally measured (−433 and −405 mV, respectively; Böhme & Schrautemeier, 1987a), the difference in potential between the vegetative and heterocyst isoforms is similar in each case (33 vs 28 mV). Whereas our value for VFd is less negative than other values reported in recent literature, it is comparable to the −355 mV potential determined for *Anabaena variabilis* ferredoxin (Cammack et al., 1977), which differs from the *Anabaena* 7120 protein at only one residue. The reduction

potential of −384 mV for VFd determined here was considered the baseline value to which all mutants were compared.

Several mutants of VFd were found to have reduction potentials comparable to wt; these included D62K, D68K, Q70K, E94D, and F65Y. The latter three mutations are fairly conservative, with F65Y maintaining side chain aromaticity, E94D retaining a negative charge with a one methylene decrease in chain length, and Q70K replacing a neutral residue with a positively charged one of slightly shorter chain length. The D62K and D68K mutations are more severe, incorporating a complete charge reversal. Despite this, their reduction potentials are not significantly altered compared to VFd. In contrast, the potentials of HFd and other mutant VFds—E94K, E94Q, F65A, F65I, and S47A—are shifted positively by as much as 93 mV, a significant change in thermodynamic properties which is unexpected for mutations at residues not directly ligated or hydrogen bonded to the [2Fe-2S] cluster or its ligands. Moreover, these thermodynamic alterations correlate directly with the kinetic data (see Table 1); that is, those VFd mutants with a less negative potential than wt show a markedly decreased rate constant for et to FNR. Clearly, this last set of mutations involves significant changes in side chain functionality. In addition, the X-ray crystal structure of VFd emphasizes the importance of residues E94 and S47; their side chains form a hydrogen bond and are part of a larger evolutionarily conserved hydrogen-bonding pattern that stabilizes the cluster binding loop of the protein (Holden et al., 1994). Interestingly, the S47T mutant, which retains the side chain hydroxyl group, was found to have a unique potential (−438 mV), shifted 56 mV more negative than wt.

In contrast to the results presented here, the reduction potentials of *Anabaena* VFd, HFd, and the E94K and F65A mutants, measured by cyclic voltammetry at a lipid bilayer-modified gold electrode, have previously been reported to be the same within an experimental error of ±15 mV (Hurley et al., 1993a, Salamon & Tollin, 1992). However, the broad nature of the current patterns for these proteins made it difficult to accurately determine the reductive and oxidative peak potentials using that methodology. More well-defined cyclic voltammograms at an activated glassy carbon electrode have been obtained by Aliverti et al. (1995a) for the [2Fe-2S] ferredoxin from spinach and three mutants at position E92 (analogous to E94 in *Anabaena*). For wt spinach Fd, direct electrochemistry produced a current−voltage response with a peak separation of 70 mV, close to the ideal value of 60 mV for a reversible one-electron process. Mutation of E92 to lysine, glutamine, or alanine both broadened the curve (interpreted as a decrease in the heterogeneous rate constant) and shifted the potential positively by 93, 73, and 78 mV, respectively. The direction and magnitude of these potential shifts are remarkably similar to those observed here for the analogous E94K and E94Q *Anabaena* mutations (+80 and +65 mV, respectively).

Reduction potentials for rFNR were determined spectrophotometrically, yielding $E_m = -323$ mV for the overall two-electron reduction and $E_1^{\circ\prime} = -331$ mV and $E_2^{\circ\prime} = -314$ mV for the individual one-electron reduction steps at pH 7.5 (see Table 3). These values agree well with those determined at a similar pH for the native protein as isolated from *Anabaena* 7119 (Sancho et al., 1988; Pueyo et al., 1991), despite the presence of six extra amino acids at the N-terminus of rFNR compared to native FNR, the latter being proteolytically cleaved during the isolation procedure [cf. Hurley et al. (1996a)]. Approximately 26% blue neutral semiquinone was thermodynamically stabilized during the potentiometric experiments. These redox results are analogous to those obtained for spinach FNR (Corrado et al., 1996). This is not surprising since the FAD conformation and environment in the crystal structures of the two native enzymes are similar (Serre et al., 1996).

Table 3: Reduction Potentials of rFNR and Fds, Alone and in Complex

		FAD of FNR			
Fd		$E_1^{\circ\prime}$ (mV)	$E_2^{\circ\prime}$ (mV)	$E_m^{\circ\prime}$ (mV)	[2Fe-2S] of Fd $E^{\circ\prime}$ (mV)
VFd	alone[a]	−331	−314	−323	−384
	complexed[b]	−291	−300	−298	−372
	ΔE	+40	+14	+25	+12
E94K	alone[a]	−331	−314	−323	−304
	complexed[b]	−291	−286	−282	−289
	ΔE	+40	+28	+41	+15
F65I	alone[a]	−331	−314	−323	−328
	complexed[b]	−277	−273	−274	−338
	ΔE	+54	+41	+49	−10
S47A	alone[a]	−331	−314	−323	−337
	complexed[b]	−269	−282	−273	−336
	ΔE	+62	+32	+50	+1

[a] Measurements were performed as described in Materials and Methods in 50 mM potassium phosphate buffer and 1 mM EDTA, pH 7.5, 4 °C, at approximately 100 mM ionic strength (the potential of VFd measured at 12 mM ionic strength was very similar to the 100 mM value; data not shown). The range of experimental error was ±1−3 mV for all VFds examined. [b] Measurements were performed as described in Materials and Methods in 4 mM potassium phosphate buffer and 1 mM EDTA, pH 7.5, 4 °C, at approximately 12 mM ionic strength. Fd and FNR were electrostatically bound in 1:1 complexes (39, 29, 14, or 26 μM each for VFd, E94K, F65I, and S47A, respectively).

Reduction Potentials of Complexed Proteins. Earlier studies of electrostatic complexes of native VFd and FNR from *Anabaena* 7119 have shown that the reduction potential of VFd shifts negatively by 15 mV while that of FNR shifts positively by 27 mV (Pueyo et al., 1992); thus, et in the physiological direction becomes thermodynamically more favorable when the proteins are bound in an intermediate complex. Similar results were obtained by Smith et al. (1981) for the spinach system. In the present system, with VFd from *Anabaena* 7120 and the rFNR from *Anabaena* 7119, the reduction potentials of both proteins are also altered upon electrostatic complex formation (see Table 3). The [2Fe-2S] cluster of VFd is shifted positively in potential by a small amount ($\Delta E = +12$ mV), while the FAD midpoint potential of rFNR is shifted positively to a greater extent ($\Delta E = +25$ mV). The net result is again an overall increase in the thermodynamic driving force for the physiological et reaction from VFd to rFNR. This increase is even greater if the potential for the first one-electron reduction of rFNR ($E_1^{\circ\prime}$) is considered; the potential for the $rFNR_{ox/sq}$ couple is shifted positively by 40 mV in the VFd−rFNR complex. This is a physiologically relevant value, inasmuch as the semiquinone state has been implicated in the catalytic cycle of FNR (Batie & Kamin, 1984; Knaff 1996), and it is also relevant to the transient et kinetics measured here in which FNR goes between the oxidized and semiquinone states.

Overall, similar potential shifts were observed for selected VFd mutants (E94K, F65I, S47A; note that these are all kinetically dead) complexed with rFNR (see Table 3). Depending on the particular VFd mutation, the potential of

Table 4: Space Groups of Crystallized Mutant VFds and Root-Mean-Square Deviations of the C^{α} Backbones of Mutant VFds Relative to Wt VFd

VFd mutant	space group	RMS deviation (Å)
D62K	$P2_12_12_1$	0.14
Q70K	$P2_12_12_1$	0.12
S47A	$P2_12_12_1$	0.25
E94K	$P3_221$	0.40
E95K	$P3_221$	0.41
D68K	$P3_221$	0.41

the [2Fe-2S] cluster is shifted a maximum of ±15 mV from its uncomplexed value. Even larger potential shifts were observed for the FAD of rFNR when the latter was electrostatically bound to mutated VFd (a range of +40 to +62 for $E_1°'$ and + 41 to +50 for E_m). These thermodynamic changes also lead to an increased driving force for et in all of the mutants examined—enough to make the VFd−rFNR et reaction isopotential (for E94K) or thermodynamically favorable (for F65I and S47A). Thus, the unfavorable positive shifts in potentials created in free VFd by these mutations can largely be overcome when the mutant VFd binds to rFNR (it should be noted that those VFd mutants which are highly impaired in their et activity with native FNR are also similarly impaired with rFNR; Hurley et al., unpublished observations). These results clearly indicate that the impairment of et activity observed with these mutants cannot be ascribed to reduction potential changes. For both wt and mutant VFds, the data point to another interesting result—that changes in the reduction potential of rFNR rather than VFd are largely responsible for promoting intracomplex et. These observations will be discussed further below.

X-ray Crystallography. Crystal structures have been determined previously for wt VFd (Rypniewski et al., 1991; Holden et al., 1994); we now report structures for the VFd mutants D62K, D68K, E94K, E95K, Q70K, and S47A. These six residues all lie at the surface of the VFd molecule. The C^{α} backbones of these mutants superimpose with that of wt Vfd with the RMS deviations given in Table 4. Figure 8 shows close-up views of the [2Fe-2S] center and the vicinity around the mutated residue for each of the mutant proteins.

Inspection of the data in Table 4 and the structures presented in Figure 8 demonstrates that none of the mutations caused any major perturbation in the VFd structure. It should be noted that the larger RMS values listed in Table 4 are for mutants that crystallized in a different space group and are most likely due to differences in crystal packing. Careful inspection of the close-up views of the regions near the mutated residues in E94K and S47A, however, does indicate that these two kinetically dead mutants are more perturbed than the other four, wt-like, mutants. This is most likely due to loss of the hydrogen bond between these two residues. In this context, it should be pointed out that structural perturbations at the C-terminus, relative to VFd, appear to be quite variable among the mutants. These do not, however, correlate with et reactivity. Thus, although the wt-like mutants Q70K and D62K have minimal perturbations in this region, the dead mutant S47A also has only small structural changes here. Furthermore, large structural changes in the C-terminal vicinity are seen in D68K (a very reactive mutant) and E95K (the mutant which is most like wt in its et behavior).

Several other structural features in this group of proteins should be noted.

(1) D62K: the native Asp 62 side chain is ordered; in the mutant, C^{γ}, C^{δ}, and C^{ϵ} of the Lys side chain are disordered.

(2) E94K: the native Glu 94 side chain is ordered; in the mutant, C^{δ}, C^{ϵ}, and N^{ζ} of the Lys side chain are disordered, probably because of the loss of the hydrogen bond to Ser 47.

(3) D68K: the native Asp 68 side chain at position C^{γ} shows a high temperature factor—the electron density for this side chain is more spread out than observed for other residues—most likely as a consequence of conformational flexibility. In the mutant, C^{γ}, C^{δ}, C^{ϵ}, and N^{ζ} of the Lys side chain are disordered.

(4) E95K: the Glu 95 side chain at positions C^{δ}, $O^{\epsilon 1}$, and $O^{\epsilon 2}$ (i.e., the carboxylate group) is disordered in the native protein; in the mutant, C^{δ}, C^{ϵ}, and N^{ζ} of the Lys side chain are disordered.

(5) Q70K and S47A: the side chains are ordered in both the native and mutant structures. Electron density maps of these regions are shown in Figure 2.

(6) Temperature factor plots (not shown) revealed no significant differences for any of the mutants relative to the wt protein. Each protein showed two regions of significantly enhanced mobility, the C-terminus (residues 94−98) and the residues 10−13. The average *B* values ranged from 27.7 A^2 (E95K and Q70K) to 34.1 A^2 (E94K).

DISCUSSION

The study of interprotein et is rooted in many interesting basic questions, which for most systems remain unanswered. These include the following: Which chemical forces (Coulombic interactions, hydrogen bonds, hydrophobic interactions/aromatic ring stacking) are most important for maintaining a functional protein−protein complex? Which protein characteristics (structure, reduction potentials) exert the most influence on the et rate constant? Are electrons transferred via fixed pathways, and how does altering these pathways (i.e., through mutagenesis) affect the rate constant? The present study incorporates kinetic, thermodynamic, and structural data in an effort to address these issues for the Fd−FNR system of the cyanobacterium *Anabaena*.

Correlations among Kinetic Properties, 3-D Structures, and Reduction Potential Measurements. As noted above, we sought to evaluate two possible explanations for the large perturbation in et reactivity observed upon the introduction of nonconservative mutations at S47, F65, and E94: (i) that the mutations significantly perturbed the 3-D structure of VFd, resulting in a nonproductive complex with FNR, and (ii) that the alteration of the [2Fe-2S] reduction potential by the mutations erected a thermodynamic barrier to intracomplex et.

The crystallographic results clearly demonstrate that structural alterations in the immediate vicinity of the [2Fe-2S] cluster do *not* occur for any of the mutants investigated here, including the kinetically dead E94K and S47A mutants. Furthermore, although some perturbations in the C-terminal region were found, the magnitude of these changes did not correlate with either et reactivity or reduction potential shifts.

The reduction potentials of the kinetically dead mutants E94K, E94Q, F65A, F65I, and S47A were all positively shifted relative to VFd (Table 1). Thus, these mutations place the [2Fe-2S] cluster in either a nearly isopotential or

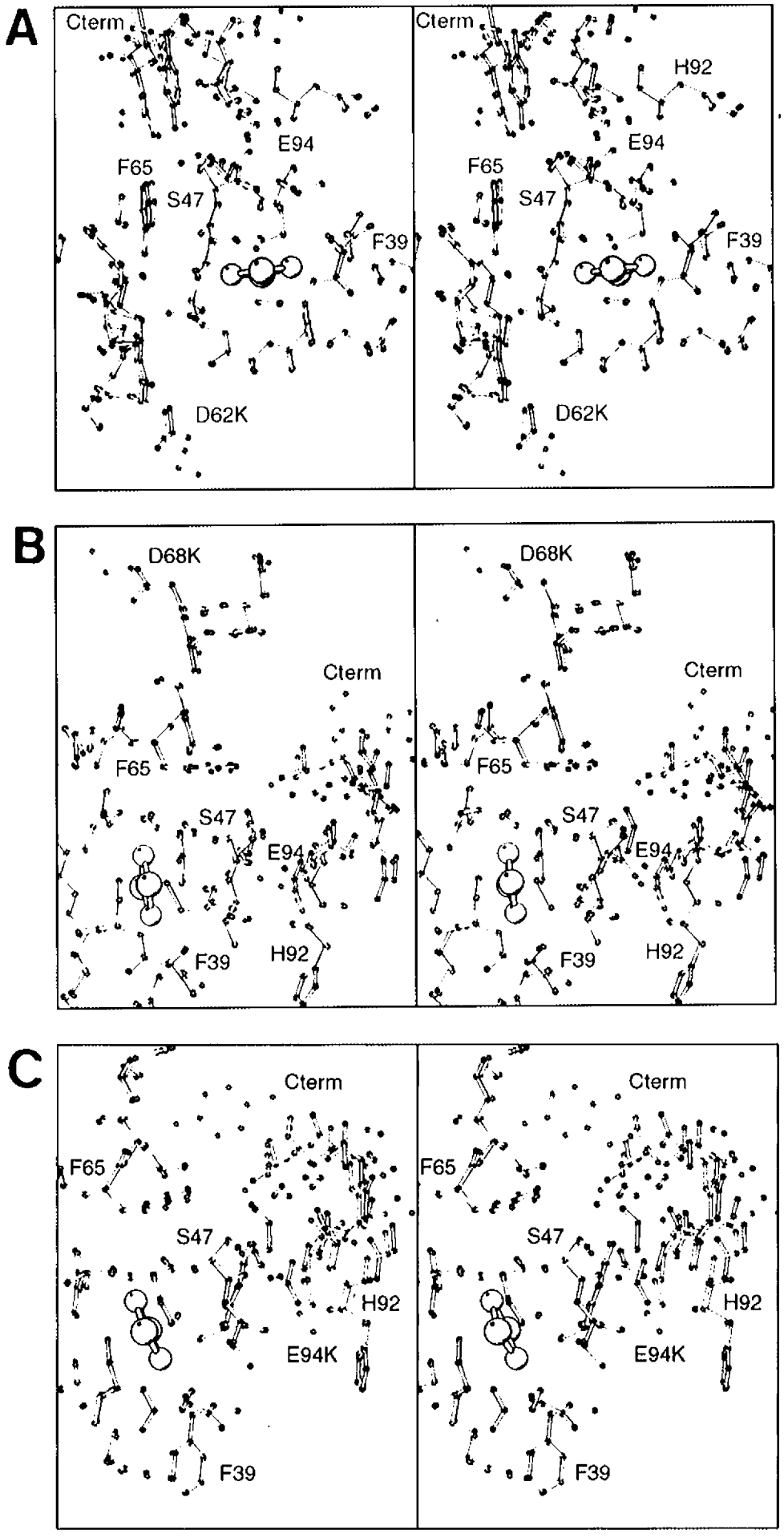
A
Cterm
E94
F65
S47
F39
D62K
Cterm
H92
E94
F65
S47
F39
D62K
B
D68K
Cterm
F65
S47
E94
F39
H92
D68K
Cterm
F65
S47
E94
F39
H92
C
Cterm
F65
S47
H92
E94K
F39
Cterm
F65
S47
H92
E94K
F39

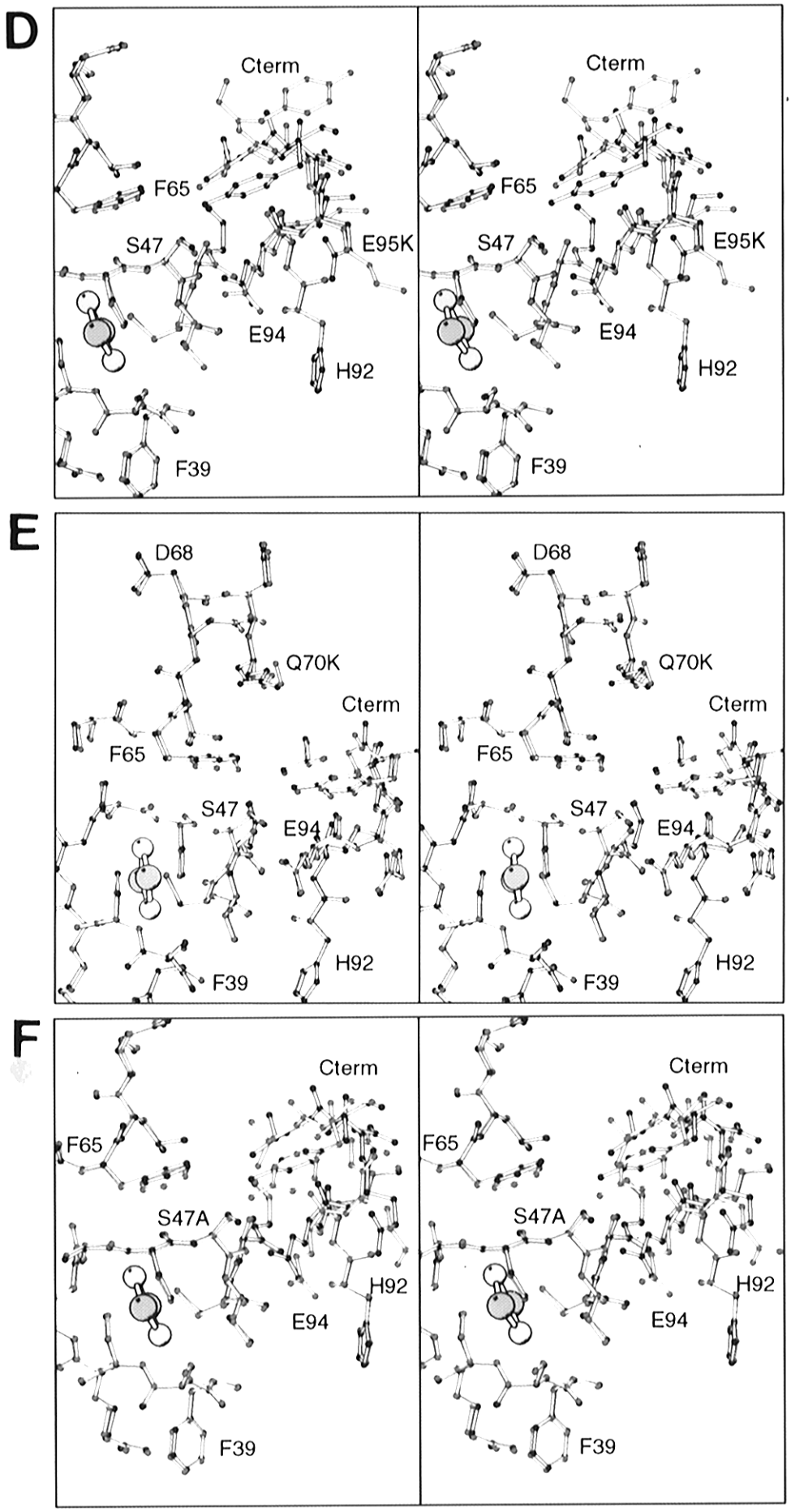

FIGURE 8: Stereoviews of the mutant VFds showing amino acid side chains in the immediate vicinity of the [2Fe-2S] cluster: (A) D62K, (B) D68K, (C) E94K, (D) E95K, (E) Q70K, and (F) S47A. The wt and mutant structures are colored black and red, respectively. The figures were prepared using MOLSCRIPT (Kraulis, 1991).

an energetically uphill position for transferring electrons to FNR. However, despite the strong correlations observed between these potential shifts in VFd and changes in et kinetics, reduction potential changes are unlikely to be the principal factor governing the loss of et reactivity in these mutants. This is due to the following considerations: (i) The experimental conditions under which the transient kinetic experiments were carried out typically involved ratios of oxidized FNR to reduced VFd of >30:1; this would easily compensate for the $\leq +93$ mV shift in potential observed with these mutants (it can be estimated that as much as 90 mV could be compensated in this way). (ii) The reduction potentials of the dead F65I (−328 mV) and S47A (−337 mV) mutants are essentially the same as that of the $FNR_{ox/sq}$ couple (−331 mV). Thus, there should be no thermodynamic barrier to their reactivity. (iii) The reduction potential of HFd (−351 mV), which is quite reactive toward FNR, is not appreciably different from those of the unreactive F65I and S47A mutants. (iv) The rFNR complexation experiments with E94K, F65I, and S47A demonstrate that, in contrast to the situation for the unbound protein partners, the proteins become either isopotential (E94K) or favorably poised for electron transfer (F65I and S47A) within the oxidized Fd/rFNR complex (Table 3). (v) E94Q, F65A, and F65I all show appreciable activity toward nitrite reductase (19%, 32%, and 55% activity, respectively) in a steady-state kinetic assay (Schmitz & Böhme, 1995), despite an apparent thermodynamic barrier to electron transfer from these mutants to the siroheme group of the reductase ($E_m = -365$ mV; Hirasawa et al., 1994).

Taken together, these results strongly suggest that more than just reduction potential determines whether or not these et reactions will occur. Despite this, we cannot completely rule out the possibility that thermodynamic differences partially account for the loss of reactivity, especially for the E94K and F65A mutants whose reduction potentials are more severely affected. However, our conclusion from these considerations is that specific protein−protein interactions, which control the mutual orientation of the proteins within the intermediate et complex and are altered by amino acid changes in the protein−protein interfacial region, are most likely the predominant factor leading to the kinetic results observed with the present set of VFd mutants.

Identification of VFd Residues Critical to the et Reaction with FNR. The kinetic experiments described above lead to five basic conclusions concerning the importance of specific surface structural features of VFd:

(1) HFd and the mutants D62K, D68K, Q70K, E94D, E95K, F65Y, and S47T essentially possess wt VFd characteristics with regard to et to FNR, whereas E94Q, E94K, F65A, F65I, and S47A are greatly impaired in this respect. On the basis of previous experiments, the HFd result is not surprising. Although HFd functions primarily in nitrogen fixation, it has been shown to be 54% as active as is VFd in an $NADP^+$ photoreduction steady-state assay (Schmitz & Böhme, 1995). This may be due in part to sequence homology between HFd and VFd in the FNR binding region; e.g., HFd contains the critical residues S47, F65, and E94 (Böhme & Haselkorn, 1988). Alternatively, the greater flexibility of HFd as revealed by NMR dynamics studies (Chae et al., 1994) may allow it to adopt a conformation suitable for docking with and transferring electrons to FNR, despite structural differences. Our observations that E94Q, F65A, and F65I mutants are appreciably less reactive toward FNR have been independently confirmed in steady-state experiments by Schmitz and Böhme (1995), who found that these mutants were all less than 5% as effective as VFd in reducing rFNR. In addition, steady-state assays of the ferredoxin-dependent glutamate synthases from spinach (M. Hirasawa and D. Knaff, personal communication) and from *Synechocystis* 6803 (Schmitz et al., 1996) yielded significantly decreased turnover numbers when VFd mutants in which F65 was replaced by nonaromatic amino acids, or in which the negative charge was eliminated at E94, were used as electron donors in place of wt VFd.

(2) We have previously shown that aromaticity at F65 (Hurley et al., 1993b) and acidity at E94 (Hurley et al., 1994) are essential for formation of a productive et complex with FNR. The kinetic studies herein identify an additional critical residue, S47, whose side chain hydroxyl group appears to be the crucial component (since S47T restores wild-type activity).

(3) Whereas mutants D62K, D68K, and Q70K have second-order rate constants comparable to wt protein at low ionic strength (Table 1), their k_{et} values are slightly smaller at high ionic strength (Table 2) and their ionic strength profiles differ from wt [Figure 4 and Hurley et al. (1995a)]. These results clearly indicate that these residues do interact with FNR during et, albeit in a noncritical manner.

(4) The same type of mutation (introduction of a positively charged lysine) at different but nearby acidic or neutral residues can result in either a kinetically dead (E94K) or a viable mutant (E95K, D62K, D68K, and Q70K), emphasizing the highly localized nature of the VFd−FNR interfacial interaction.

(5) The kinetic inactivity of dead mutants is not due to poor binding, as shown by K_d determinations. Rather, the problem is inefficiency in the et step.

Functional Importance of a Hydrogen Bond between E94 and S47. The kinetic and thermodynamic results for the nonconservative E94 and S47 mutants suggest that the loss of the H-bond between these residues (Holden et al., 1994) is an important factor in controlling *both* reactivity *and* the iron−sulfur cluster potential. This bond is part of a larger hydrogen-bonding network that tethers the [2Fe-2S] cluster to the C-terminal α-helix, helping to stabilize an otherwise highly flexible region of the protein (Holden et al., 1994). Disruption of this important network could block the et pathway out of the ferredoxin, as well as perturb the normal binding modes between VFd and FNR that allow formation of a productive et complex. In this context, it is significant that the S47T mutant, although somewhat less reactive than VFd, is far from being inactive. Although we do not have a crystal structure for this mutant, it seems likely that the H-bonding capability at this position is retained. The relatively small decrease in reactivity observed with the S47T mutant may result from the increased bulk of the threonine side chain, which could influence the topography of the protein−protein interface in the intermediate complex, or induce changes in the length or directionality of the hydrogen bond between residues 47 and 94. Removal of the side chain hydroxyl moieity in S47A raised the VFd potential by approximately 50 mV, while mutation to the slightly larger threonine in S47T actually lowered the potential by the same amount. This sensitivity is not entirely unexpected, due to the sequential and three-dimensional proximity of this residue to the cluster cysteines 46 and 49 and the functionally important residue E94. Polar side chains are expected to

make significant contributions to the electrostatic potential of iron−sulfur clusters, based on the theoretical calculations of Swartz et al. (1996) for rubredoxins and HiPIPs. Interestingly, a conserved hydrogen-bonding network in cytochromes *c* has been postulated to be a factor in maintaining the reduction potentials in this class of et proteins (Caffrey et al., 1991). Although the 50 mV negative potential shift in S47T adds considerable driving force to the S47T/FNR reaction, the et rate constant does not reflect this change (Tables 1 and 4); however, the possibility that this potential is shifted positively in the protein−protein complex cannot be discounted. This latter effect was observed for both VFd and E94K. Additional complexation experiments are underway to investigate this. Regardless, this combination of structural and functional data identifies S47 (and presumably its hydrogen-bonding capability) as a critical component of the et process between VFd and FNR.

Another conserved residue, T48, participates in the same conserved hydrogen-bonding network as E94 and S47. The hydroxyl side chain of T48 is within hydrogen-bonding distance (3.4 Å) to one of the bridging inorganic sulfurs of the cluster (Holden et al., 1994). However, in contrast to S47A, removal of the side chain hydroxyl group at this position via the mutation T48A does not alter the VFd reduction potential (Weber-Main et al., in preparation) and results in only slightly perturbed kinetic properties compared to VFd (the k_{et} for et to FNR is smaller by a factor of 2, not nearly as dramatic as the orders of magnitude decrease in rate constant observed for S47A; Hurley et al., unpublished data). Thus, as demonstrated for the E94K and E95K mutants, the same type of functional change just one residue removed can either retain wt properties or create a mutant with critically altered functional properties. This emphasizes the very specific complementarity between VFd and FNR required for formation of a productive complex capable of supporting efficient et.

Influence of Aromaticity at F65 on VFd Reduction Potential. The F65 mutations demonstrate the importance of aromaticity at this VFd residue for maintaining both efficient kinetic activity with its biological partner FNR [previously discussed in Hurley et al. (1993b)] and a favorably low intrinsic reduction potential. While no crystal structures are available for mutations at this site, we can hypothesize that the aromatic ring imparts steric properties which, if removed, appreciably perturb the [2Fe-2S] cluster environment and subsequently alter its reduction potential. Mutation of F65 to alanine shifted the potential 37 mV less negative than the mutation to isoleucine. It is possible that, compared to alanine, the greater hydrophobicity and increased bulk of isoleucine more effectively maintains the structural integrity of the protein, resulting in redox properties closer to that of wild-type. Any further structural insights must await elucidations of the structures of these F65 mutants. Interestingly, while highly conserved in many photosynthetic [2Fe-2S] Fds (Rogers, 1987; Matsubara & Saeki, 1992; Matsubara & Hase, 1983), F65 is a methionine in several bacterial and vertebrate Fds, such as bovine adrenodoxin (Okamura et al., 1985) and putidaredoxin (Peterson et al., 1990), which have characteristically higher reduction potentials than their photosynthetic counterparts.

In general, aromatic residues are found only sparingly in the sequences of Fds, yet those present are often highly conserved and as such have been the target of several mutagenesis investigations. In *Azotobacter vinelandii* Fd I (*Av*FdI), mutations have been introduced at two buried phenylalanine residues in close proximity to the [4Fe-4S] cluster (Shen et al., 1994). No change in potential was observed for the F25Y mutation in which aromaticity was preserved, similar to our results for the F65Y *Anabaena* mutant. In contrast, the F25I mutation in *Av*FdI shifted the potential 20 mV negatively. This mutant also exhibited perturbed ^{1}H-NMR and EPR spectra, reflecting a number of steric clashes and conformational shifts observed in its X-ray crystal structure. In *Chromatium vinosum* HiPIP, several conserved aromatic core residues have been mutated to charged, polar, and nonaromatic hydrophobic amino acids (Agarwal et al., 1995; Soriano et al., 1996). For most mutants, the changes in the [4Fe-4S] cluster potential were minimal, despite demonstrated increases in solvent accessibility for some Y19 mutants (Li et al., 1996). A few larger shifts were reported, specifically for F66N (+47mV), but otherwise the authors dismissed these as "minimal changes", and accounted for the consistency in potential by demonstrating a balance of favorable entropies of reduction and less favorable reaction enthalpies (Soriano et al., 1996). The relatively small influence of aromatic residues on [Fe-S] cluster potential in these and other systems (Quinkal et al., 1996) have led investigators to conclude that these residues primarily serve to maintain protein stability, most likely by excluding solvent from the cluster region. In this context, it is interesting that both the F65A and F65I *Anabaena* mutants are significantly less stable to guanidine hydrochloride denaturation than are either VFd or the F65Y and F65W mutants (Hurley et al., 1995b). However, the large potential shifts induced by removal of aromaticity at this site (+56 and +93 mV for F65I and F65A, respectively) suggest a thermodynamic role for such residues in [2Fe-2S] Fds. Further insight into the origin of this thermodynamic control would be gained by structural characterization of the F65A/I mutants. Unfortunately, X-ray structures could not be obtained in the present study, inasmuch as suitable crystals were not forthcoming.

Comparison of et Reactivity of E → K Mutations in Anabaena VFd and the [2Fe-2S] Fd from Spinach. From steady-state studies of the spinach Fd−spinach FNR system, in which site-directed mutagenesis was used to change the E92 Fd residue (which is homologous to E94 in *Anabaena* Vfd), it was concluded that mutation to Lys does not significantly impair et (Aliverti et al., 1995a). However, the assay used was a nonphysiological process which proceeds in the opposite direction, in which Fd catalyzes et from NADPH to cytochrome *c* via FNR; it is not known what the rate-determining step is in this series of reactions. In a later study of the physiological reaction (Piubelli et al., 1996), it was demonstrated that the E92 mutants in spinach Fd are not as efficient as wt Fd in transferring electrons from photosystem I to membrane-bound FNR. Thus, E92Q, E92A, and E92K were respectively 58%, 53%, and 30% as efficient as wt in transferring electrons to FNR. Although this was attributed to their less negative reduction potentials (Aliverti et al., 1995a), it is possible that the potential of spinach FNR is positively shifted in the interprotein complex as we have observed for the *Anabaena* system, thereby thermodynamically compensating for the positive shift in the E92 Fd mutants. Again, it must be pointed out that the rate-limiting process in these complex steady-state assay systems is not clearly defined, and thus the observed rates may not directly reflect the et process from Fd to FNR. Alternatively,

species differences may be operative here. Indeed, Walker et al. (1991) found significant differences between the spinach and *Anabaena* systems with regard to ionic strength effects on the VFd−FNR et reaction. This may be a consequence of the appreciable differences which exist between the charged residue distributions in these two sets of proteins.

Influence of E94 on Reduction Potentials of the [2Fe-2S] Fd from Anabaena 7120 and Spinach. For *Anabaena* and spinach, the effect of analogous mutations (at positions E94 and E92, respectively) on the intrinsic thermodynamic reduction potentials of their [2Fe-2S] Fds are strikingly similar. For both systems, mutation of the negatively charged Glu to Lys or Gln positively shifts the Fd reduction potential by approximately 65−95 mV (Aliverti et al., 1995a). Thus, this conserved residue appears to be an important site of reduction potential control in both cyanobacterial and higher plant [2Fe-2S] Fds. It is noteworthy that the spinach E92K/Q/A mutations apparently result in an altered cluster geometry, as evidenced by their perturbed EPR spectra (Aliverti et al., 1995a). The near wt potential of the E94D *Anabaena* mutant suggests that either the negative charge at this position or its ability to form hydrogen bonds with S47 and an ordered water molecule via its acidic side chain (Holden et al., 1994) help to maintain the low reduction potential of the [2Fe-2S] cluster.

Molecular modeling investigations of various iron−sulfur proteins including [2Fe-2S] Fds have theoretically addressed the influence of charged residues on reduction potentials (Jensen et al., 1994; Stephens et al., 1996). These calculations predict that side chain charges can contribute to variations in reduction potentials on the order of tens of millivolts, although other factors, including the interaction of the backbone amide groups with the cluster, appear to be more important. Swartz et al. (1996) calculated the classical electrostatic potential of the iron−sulfur clusters of rubredoxins and, using molecular dynamics simulations of surrounding solvent water, demonstrated that water largely dampens the contribution of charged side chains. Shen et al. (1993, 1994) examined this issue experimentally for *Av*FdI which contains one [3Fe-4S] cluster and one [4Fe-4S] cluster. Neutralization of surface acidic residues or introduction of acidic sites via site-directed mutagenesis had no appreciable effect on the reduction potentials of the clusters. Only mutants D15N (Shen et al., 1993) and H35D/D41H (Shen et al., 1994) increased the potential, and then only by approximately 20 mV, compared to the >65 mV shifts observed here for point mutations at a surface acidic site. Thus, the magnitudes of the *Anabaena* E94K/Q potential shifts observed in this work seem unusually large for Fds. While the enhanced ease of reduction of these mutants may be due to removal of a negative charge near the cluster, our results also show that introduction of a positively charged Lys at E95, D62, D68, and Q70 does not alter the redox properties of the cluster. Thus, either factors other than charge effects are responsible for the large E94K/Q potential shifts or the specific location and environment of the charged residue (including, for example, distance from the cluster, solvent exposure, local dielectric constant) must be carefully considered in predicting its ability to tune the cluster potential. In fact, there appears to be an approximate correlation between reduction potential and distance from the [2Fe-2S] cluster for the VFd mutants. Thus, the distances from Fe1 of the cluster to $O^{\epsilon 1}$ of E94, $O^{\epsilon 1}$ of E95, $O^{\delta 1}$ of D62, $O^{\delta 1}$ of D68, and $N^{\epsilon 2}$ of Q70 are 8.0, 13.4, 12.5, 17.5, and 13.2 Å, respectively. Thus, within this group of residues, E94 is significantly closer to the cluster than the others, and its charge-reversal mutation results in the largest redox potential perturbation.

Induction of Positive Potential Shifts in FNR by the Binding of VFd and Mutants. The observed shifts in the reduction potential of the FAD of *Anabaena* rFNR induced by the binding of wt or mutant VFd (Table 3) are not unprecedented. The presence or absence of a [2Fe-2S] cluster has been shown to influence the potential of flavin cofactors in both phthalate dioxygenase reductase (PDR) (Gassner & Ballou, 1995) and CDP-6-deoxy-L-*threo*-D-*glycero*-4-hexulose-3-dehydrase reductase (E_3) (Burns et al., 1996). Both PDR and E_3 belong to the FNR family of flavoprotein reductases by virtue of their highly conserved flavin and pyridine nucleotide binding motifs (Ploux et al., 1995; Karplus et al., 1991) and are among the few members whose redox properties have been characterized in detail. The [2Fe-2S] and FAD domains of PDR and E_3 occur within the same polypeptide chain, in contrast to the separate [2Fe-2S] Fd partner of FNR. When the PDR holoenzyme was proteolytically cleaved to produce a truncated form of PDR minus the iron−sulfur center, the potential of the $FMN_{ox/sq}$ couple remained the same (−174 mV), but the $FMN_{sq/red}$ potential increased by approximately 50 mV (from −285 to −235 mV) (Gassner & Ballou, 1995). In other words, the presence of the [Fe-S] cluster in the holoenzyme caused a negative potential shift in $E_2^{\circ\prime}$, postulated to arise from destablization of the fully reduced anionic flavin by the negative charge associated with the reduced [2Fe-2S] cluster. For E_3, the [2Fe-2S] cluster was removed by treatment with mersalyl acid (Burns et al., 1996). The presence of the iron−sulfur center in the holoenzyme of E_3, compared to the apoFeS form, shifted the $FAD_{ox/sq}$ potential negatively by 16 mV and the $E_{sq/red}$ potential positively by 48 mV. For both E_3 and PDR, $E_2^{\circ\prime}$ was affected the most, though the shifts were in opposite directions. This may be due to their distinct domain organizations (Burns et al., 1996).

For *Anabaena* rFNR, the data reported herein show that the "presence" of the [2Fe-2S] center in the VFd−rFNR complex shifts both $E_1^{\circ\prime}$ and $E_2^{\circ\prime}$ positively. The direction of the $E_2^{\circ\prime}$ shift makes this system more like E_3 than PDR. However, the magnitude of the FAD potential shifts in VFd−rFNR is greatest for $E_1^{\circ\prime}$, which is a significant difference between rFNR and the other reductases. The distinct redox properties of the VFd−rFNR system most likely have mechanistic and structural origins. For example, in E_3, PDR, and most other FNR-like reductases, electrons are proposed to shuttle from a pyridine nucleotide to flavin to a one-electron acceptor such as a [2Fe-2S] cluster. FNR is unusual in that the physiological direction of electron flow is in the opposite direction: from [2Fe-2S] to flavin, with the net production of NADPH. Despite this functional difference, both FNR and PDR can exploit the presence of a [2Fe-2S] cluster to appropriately shift their flavin potentials (albeit in opposite directions) to increase the overall thermodynamic driving force for et. The E_3 case is unusual in that, at pH 7.5, et between the flavin and iron−sulfur center of the holoenzyme is actually thermodynamically unfavorable. An increase in pH to 8.4 makes et feasible, suggesting prototropic control (Burns et al., 1996).

While no crystal structure exists for a VFd−FNR complex, a putative model has been constructed by superposition of

the spinach FNR and *Anabaena* VFd structures onto the equivalent PDR domains (Correll et al., 1993). However, this model conflicts with the cross-linking and mutagenesis data (Hurley et al., 1993a; Vieira et al., 1986; Zanetti et al., 1988), which place the C-terminus of VFd (including the critical E94 residue in *Anabaena* Fd) near the VFd−FNR interface. This suggests that the true VFd−FNR interface is quite different from the PDR domain interface and cannot be accurately modeled by a simple superposition (Correll et al., 1993). Thus, structural differences between the Fd−FNR and PDR interfaces, though not yet well defined, may account for the distinct influences of a [2Fe-2S] cluster on the flavins of FNR and PDR.

Conceivably, wt or mutant VFd binding could induce any number of conformational changes in FNR—evidenced by changes in absorbance, circular dichroism, and fluorescence spectra (Knaff & Hirasawa, 1991)—resulting in an altered flavin environment and unique redox properties. For example, $\pi-\pi$ stacking interactions between the FAD and the active site tyrosines of Y79, Y104, and Y303 (Serre et al, 1996) could be perturbed. Zhou and Swenson (1996) invoked such an effect to explain the altered redox properties of tyrosine mutants in flavodoxin. Perturbation of $\pi-\pi$ interactions could also disrupt electronic coupling between the two redox centers of VFd and FNR, thereby explaining the kinetic inactivity of some of the VFd mutants. This may prove to be particularly pertinent for the F65 mutants, in which the importance of maintaining an aromatic ring at this position for efficient et is clearly evident.

For the E94K−rFNR complex, the presence of a new positively charged lysine in the interfacial region could electrostatically stabilize the anionic hydroquinone. The recent literature contains several examples of flavoprotein redox properties modulated by the presence of charged residues near the active site. For *Desulfovibrio vulgaris* flavodoxin, potential shifts of >180 mV in the $FMN_{sq/red}$ couple have been reported after incorporation of positively charged residues in place of an active site Tyr (Swenson & Krey, 1994). Furthermore, neutralization of several acidic residues located within 13 Å of the N(1) of the flavin cofactor also shifted the potential, with an average contribution of 15 mV per substitution (Zhou & Swenson, 1995). For MCAD and the analogous short-chain enzyme (SCAD), binding studies with natural substrate/product or transition state analogs support the hypothesis that even partial positive charges induced on a binding ligand in the active site can significantly shift the reduction potential of flavins—over 100 mV positive for MCAD bound to natural substrate/product couple (Fink et al., 1986; Lenn et al., 1990; Johnson et al., 1995; Becker et al., 1994). While electrostatic effects may indeed play a role in modulating the redox properties of rFNR bound to VFd, the data herein are inconclusive, as similar shifts are observed whether E94K, wt, or one of the other two dead mutants, F65I and S47A, is the binding partner. Clearly, a greater understanding of the origin of VFd's influence on the redox properties of FNR would be gained by structure−reduction potential correlation experiments on FNR itself (such as characterization of the S96V and S96G mutants of spinach FNR; Aliverti et al., 1995b) and determination of an X-ray crystal structure for the actual VFd−rFNR complex.

From the data presented above, it can be concluded that, despite the inability of E94K, F65I, and S47A VFd mutants to efficiently transfer an electron to native FNR, all are still capable of forming tight complexes with the flavoprotein (albeit nonproductive ones) and inducing a thermodynamically favorable change in its redox properties. The changes in rFNR reduction potential are qualitatively similar whether wt or mutant VFd is bound, in that both $E_1^{o\prime}$ and $E_2^{o\prime}$ are positively shifted in all cases. However, quantitative differences are observed; all three mutants shift both redox couples to a larger extent than wt, with the magnitude of the shifts being dependent on the particular mutation. Furthermore, the potentials of the [2Fe-2S] centers in the mutant Fds are also shifted in unique ways from wt (both qualitatively and quantitatively) in the protein−protein complex. Taken in combination, these results support our hypothesis that mutation of these critical VFd residues perturbs the normal docking modes between VFd and native FNR, leading to stable but distinctly different complexes with unique structural and functional properties.

ACKNOWLEDGMENT

The expert technical assistance of Rameh Hafezi in various aspects of this work is greatly appreciated.

SUPPORTING INFORMATION AVAILABLE

Tables of intensity statistics (Table S-1) and of refinement statistics (Table S-2) pertaining to the X-ray crystal structures of the ferredoxin mutants D62K, D68K, E94K, E95K, Q70K, and S47A (6 pages). Ordering information is given on any current masthead page.

REFERENCES

Agarwal, A., Li, D., & Cowan, J. A. (1995) *Proc. Natl. Acad. Sci. U.S.A. 92*, 9440−9444.
Alam, J., Whitaker, R. A., Krogman, D. W., & Curtis, S. E. (1986) *J. Bacteriol. 168*, 265−1271.
Aliverti, A., Hagen, W. R., & Zanetti, G. (1995a) *FEBS Lett. 368*, 220−224.
Aliverti, A., Bruns, C. M., Pandini, V. E., Karplus, P. A., Vanoni, M. A., Curti, B., & Zanetti, G. (1995b) *Biochemistry 34*, 8371−8379.
Arnon, D. I., & Buchanan, B. B. (1971) *Methods Enzymol. 23*, 413−440.
Ausubel, F. M., Brent, R., Kingston, R. E., Moore, D. D., Seidman, J. G., Smith, J. A., & Struhl, K., Eds. (1989) *Current Protocols in Molecular Biology*, John Wiley & Sons, New York.
Batie, C. J., & Kamin, H. (1984) *J. Biol. Chem. 259*, 11976−11985.
Becker, D. F., Fuchs, J. A., & Stankovich, M. T. (1994) *Biochemistry 33*, 7082−7087.
Bhattacharyya, A. K., Tollin, G., Davis, M., & Edmondson, D. E. (1983) *Biochemistry 22*, 5270−5279.
Böhme, H., & Schrautemeier, B (1987a) *Biochim. Biophys. Acta 891*, 1−7.
Böhme, H., & Schrautemeier, B (1987b) *Biochim. Biophys. Acta 891*, 115−120.
Böhme, H., & Haselkorn, R. (1988) *Mol. Gen. Genet. 214*, 278−285.
Böhme, H., & Haselkorn, R (1989) *Plant Mol. Biol. 12*, 667−672.
Burns, K. D., Pieper, P. A., Liu, H.-w., & Stankovich, M. T. (1996) *Biochemistry 35*, 7879−7889.
Caffrey, M. S., Daldal, F., Holden, H. M., & Cusanovich, M. A. (1991) *Biochemistry 30*, 4119−4125.
Cammack, R., Rao, K. K., Bargeron, C. P., Hutson, K. G., Andrew, P. W., & Rogers, L. J. (1977) *Biochem. J. 168*, 205−209.
Canters, G. W., & Dennison, C. (1995) *Biochimie 77*, 506−515.
Chae, Y. K., Abildgaard, F., Moosberry, E. S., & Markley, J. L. (1994) *Biochemistry 33*, 3287−3295.
Cheng, H., Xia, B., Reed, G. H., & Markley, J. L. (1994) *Biochemistry 33*, 3155−3164.
Clark, W. M. (1960) in *Oxidation−Reduction Potentials of Organic Systems*, Williams and Wilkins, New York.

Corrado, M. E., Aliverti, A., Zanetti, G., & Mayhew, S. G. (1996) *Eur. J. Biochem. 239*, 662−667.
Correll, C. C., Ludwig, M. L., Bruns, C. M., & Karplus, P. A. (1993) *Protein Sci. 2*, 2112−2133.
Curry, W. B., Grabe, M. D., Kurnikov, I. V., Skourtis, S. S., Beratan, D. N., Regan, J. J., Aquino, A. J. A., Beroza, P., & Onuchic, J. N. (1995) *J. Bioenerg. Biomembr. 27*, 285−293.
De Pascalis, A. R., Jelesarov, I., Ackermann, F., Koppenol, W. H., Hirasawa, M., Knaff, D. B., & Bosshard, H. R. (1993) *Protein Sci. 2*, 1126−1135.
Duggleby, R. G. (1981) *Anal. Biochem. 110*, 9−18.
Durham, B., Fairris, J. L., McLean, M., Millett, F., Scott, J. R., Sligar, S. G., & Willie, A. (1995) *J. Bioenerg. Biomembr. 27*, 331−340.
Fillat, M. F., Borrias, W. E., & Weisbeek, P. J. (1990) in *Flavins and Flavoproteins 1990* (Curti, B., Ronchi, S., & Zanetti, G., Eds.) pp 445−448, Walter de Gruyter & Co., Berlin.
Fillat, M. F., Pacheco, M. L., Peleato, M. L., & Gomez-Moreno, C. (1994) in *Flavins and Flavoproteins 1993* (Yagi, K., Ed.) pp 447−450, Walter de Gruyter & Co., Berlin.
Fink, C. W., Stankovich, M. T., & Soltysik, S. (1986) *Biochemistry 25*, 6637−6643.
Gassner, G. T., & Ballou, D. P. (1995) *Biochemistry 34*, 13460−13471.
Gomez-Moreno, C., Martinez-Júlvez, M., Fillat, M. F., Hurley, J. K., & Tollin G. (1995) in *Photosynthesis: from Light to Biosphere* (Mathis, P., Ed.) Vol. II, Kluwer Academic Press Publishers, Dordrecht, The Netherlands.
Hirasawa, M., Tollin, G., Salamon, Z., & Knaff, D. B. (1994) *Biochim. Biophys. Acta 1185*, 336−345.
Holden, H. M., Jacobson, B. L., Hurley, J. K., Tollin, G., Oh, B.-H., Skjeldal, L., Chae, Y. K., Cheng, H., Xia, B., & Markley, J. L. (1994) *J. Bioenerg. Biomembr. 26*, 67−88.
Hurley, J. K., Salamon, Z., Meyer, T. E., Fitch, J. C., Cusanovich, M. A., Markley, J. L., Cheng, H., Xia, B., Chae, Y. K., Medina, M., Gomez-Moreno, C., & Tollin, G. (1993a) *Biochemistry 32*, 9346−9354.
Hurley, J. K., Cheng, H., Xia, B., Markley, J. L., Medina, M., Gomez-Moreno, C., & Tollin, G. (1993b) *J. Am. Chem. Soc. 115*, 11698−11701.
Hurley, J. K., Medina, M., Gomez-Moreno, C., & Tollin, G. (1994) *Arch. Biochem. Biophys. 312*, 480−486.
Hurley, J. K., Fillat, M., Gomez-Moreno, C., & Tollin, G. (1995a) *Biochimie 77*, 539−548.
Hurley, J. K., Caffrey, M. S., Markley, J. L., Cheng, H., Xia, B., Chae, Y. K., Holden, H. M., & Tollin, G. (1995b) *Protein Sci. 4*, 58−64.
Hurley, J. K., Fillat, M. F., Gomez-Moreno, C., & Tollin, G. (1996a) *J. Am. Chem. Soc., 118*, 5526−5531.
Hurley, J. K., Schmeits, J. L., Genzor, C., Gomez-Moreno, C., & Tollin, G. (1996b) *Arch. Biochem. Biophys. 333*, 243−250.
Jacobson, B. L., Chae, Y. K., Böhme, H., Markley, J. L., & Holden, H. M. (1992) *Arch. Biochem. Biophys. 294*, 279−281.
Jacobson, B. L., Chae, Y. K., Markley, J. L., Rayment, I., & Holden, H. M. (1993) *Biochemistry 32*, 6788−6793.
Jensen, G. M., Warshel, A., & Stephens, P. J. (1994) *Biochemistry 33*, 10911−10924.
Johnson, B. D., Mancini-Samuelson, G. J., & Stankovich, M. T. (1995) *Biochemistry 34*, 7047−7055.
Jones, T. A. (1985) *Methods Enzymol. 115*, 157−171.
Kabsh, W. (1988a) *J. Appl. Crystallogr. 21*, 67−71.
Kabsh, W. (1988b) *J. Appl. Crystallogr. 21*, 916−924.
Karplus, P. A. (1991) in *Flavins and Flavoproteins 1990* (Curti, B., Ronchi, S., & Zanetti, G., Eds.) pp 449−455, Walter de Gruyter & Co., Berlin.
Karplus, P. A., Daniels, M. J., & Herriott, J. R. (1991) *Science 251*, 60−66.
Knaff, D. B. (1996) in *Oxygenic Photosynthesis: The Light Reactions* (Ort, D. R., & Yocum, C. F., Eds.) pp 333−361, Kluwer Academic Publishers, Dordrecht.
Knaff, D. B., & Hirasawa, M. (1991) *Biochim. Biophys. Acta 1056*, 93−125.
Kostic, N. M. (1991) in *Metal Ions in Biological Systems* (Sigel, H., & Sigel, A., Eds.) Chapter 4, pp 129−182, Marcel Dekker, Inc., New York.
Kraulis, P. J. (1991) *J. Appl. Crystallogr. 24*, 946−950.
Kunkel, T. A., Roberts, J. D., & Zakour, R. A. (1987) *Methods Enzymol. 154*, 367−372.
Lenn, N. D., Stankovich, M. T., & Liu, H.-W. (1990) *Biochemistry 29*, 3709−3715.
Li, D., Agarwal, A., & Cowan, J. A. (1996) *Inorg. Chem. 35*, 1121−1125.
Lovenberg, W., Ed. (1973) *Iron−Sulfur Proteins*, Vol. I, Academic Press, New York.
Lovenberg, W., Ed. (1974) *Iron−Sulfur Proteins*, Vol. II, Academic Press, New York.
Lovenberg, W., Ed. (1977) *Iron−Sulfur Proteins*, Vol. III, Academic Press, New York.
Massey, V., & Hemmerich, P. (1978) *Biochemistry 17*, 9−16.
Matsubara, H., & Hase, T. (1983) in *Proteins and Nucleic Acids in Plant Systematics* (Jensen, U., & Fairbrothers, D. E., Eds.) pp 168−181, Springer-Verlag, Berlin.
Matsubara, H., & Saeki, K. (1992) *Adv. Inorg. Chem. 38*, 223−280.
Mauk, A. G., Mauk, M. R., Moore, G. R., & Northrup, S. H. (1995)) *J. Bioenerg. Biomembr. 27*, 311−330.
Mayerle, J. J., Frankel, R. B., Holm, R. H., Ibers, J. A., Phillips, W. D., & Weiher, J. F. (1973) *Proc. Natl. Acad. Sci. U.S.A. 70*, 2429−2433.
McLendon, G., & Hake, R. (1992) *Chem. Rev. 92*, 481−490.
Millet, F., Miller, M. A., Geren, L., & Durham, B. (1995) *J. Bioenerg. Biomembr. 27*, 341−351.
Moser, C. C., Keske J. M., Warncke, K., Farid, R. S., & Dutton, P. L. (1992) *Nature 355*, 796−802.
Moser, C. C., Page, C. C., Farid, R., & Dutton, P. L. (1995) *J. Bioenerg. Biomembr. 27*, 263−274.
Moulis, J. M., & Davasse, V. (1995) *Biochemistry 34*, 16781−16788.
Navaza, J. (1987) *Acta Crystallogr. A43*, 645−653.
Okamura, T., John, M. E., Zuber, M. X., Simpson, E. R., & Waterman, M. R. (1985) *Proc. Natl. Acad. Sci. U.S.A. 82*, 5705−5709.
Peterson, J. A., Lorence, M. C., & Amarneh, B. (1990) *J. Biol. Chem. 265*, 6066−6073.
Piubelli, L., Aliverti, A., Bellintani, F., & Zanetti, G. (1996) *Eur. J. Biochem. 236*, 465−469.
Ploux, O. P., Lei, Y., Vatanen, K., & Liu, H.-w. (1995) *Biochemistry 34*, 4159−4168.
Przysiecki, C. T., Bhattacharyya, A. K., Tollin, G., & Cusanovich, M. A. (1985) *J. Biol. Chem. 260*, 1452−1458.
Pueyo, J. J., & Gomez-Moreno, C. (1991) *Prep. Biochem. 21*, 191−204.
Pueyo, J. J., Gomez-Moreno, C., & Mayhew, S. G. (1991) *Eur. J. Biochem. 202*, 1065−1071.
Pueyo, J. J., Revilla, C., Mayhew, S. G., & Gomez-Moreno, C. (1992) *Arch. Biochem. Biophys. 294*, 367−372.
Quinkal, I., Kyritsis, P., Kohzuma, T., Im, S.-C., Sykes, A. G., & Moulis, J.-M. (1996) *Biochim. Biophys. Acta 1295*, 201−208.
Rogers, L. J. (1987) in *The Cyanobacteria* (Fay, P., & Van Baalen, C., Eds.) pp 35−66, Elsevier Science Publishers, Amsterdam.
Rypniewski, W. R., Breiter, D. R., Benning, M. M., Wesenberg, G., Oh, B.-H., Markley, J. L., Rayment, I., & Holden, H. M. (1991) *Biochemistry 30*, 4126−4131.
Salamon, Z., & Tollin, G. (1992) *Bioelectrochem. Bioenerg. 27*, 381−391.
Sambrook, J., Fritsch, E. F., & Maniatis, T. (1989) *Molecular Cloning, A Laboratory Manual*, Cold Spring Harbor Laboratory Press, Plainview, N.Y.
Sancho, J., Peleato, M. L., Gomez-Moreno, C., & Edmondson, D. E. (1988) *Arch. Biochem. Biophys. 260*, 200−207.
Schmitz, S., & Böhme, H. (1995) *Biochim. Biophys. Acta 1231*, 335−341.
Schmitz, S., Navarro, F., Kutzki, C. K., Florencio, F. J. & Böhme, H. (1996) *Biochim. Biophys. Acta 1277*, 135−140.
Serre, L., Vellieux, F. M. D., Medina, M., Gomez-Moreno, C., Fontecilla-Camps, J. C., & Frey, M. (1996) *J. Mol. Biol. 263*, 20−39.
Shen, B., Martin, L. L., Butt, J. N., Armstrong, F. A., Stout, C. D., Jensen, G. M., Stephens, P. J., La Mar, G. N., Gorst, C. M., & Burgess, B. K. (1993) *J. Biol. Chem. 268*, 25928−25939.
Shen, B., Jollie, D. R., Stout, C. D., Diller, T. C., Armstrong, F. A., Gorst, C. M., La Mar, G. N., Stephens, P. J., & Burgess, B. K. (1994) *J Biol. Chem. 269*, 8564−8575.

Simondsen, R. P., & Tollin, G. (1983) *Biochemistry 22*, 3008−3016.
Simondsen, R. P., Weber, P. C., Salemme, F. R., & Tollin, G. (1982) *Biochemistry 21*, 6366−6375.
Smith, J. M., Smith, W. H., & Knaff, D. B. (1981) *Biochim. Biophys. Acta 635*, 405−411.
Soriano, A., Li, D., Bian, S., Agarwal, A., & Cowan, J. A. (1996) *Biochemistry 35*, 12479−12486.
Stankovich, M. T. (1980) *Anal. Biochem. 109*, 295−308.
Stankovich, M. T., & Fox, B. (1983) *Biochemistry 22*, 4466−4472.
Stephens, P. J., Jollie, D. R., & Warshel, A. (1996) *Chem. Rev. 96*, 2491−2513.
Swartz, P. D., Beck, B. W., & Ichiye, T. (1996) *Biophys. J. 71*, 2958−2969.
Swenson, R. P., & Krey, G. D. (1994) *Biochemistry 33*, 8505−8514.
Tollin, G. (1995) *J. Bioenerg. Biomembr. 27*, 303−309.
Tollin, G., & Hazzard, J. T. (1991) *Arch. Biochem. Biophys. 287*, 1−7.
Tollin, G., Hurley, J. K., Hazzard, J. T., & Meyer, T. (1993) *Biophys. Chem. 48*, 259−279.
Tronrud, D. E., Ten Eyck, L. F., & Matthews, B. W. (1987) *Acta Crystallogr. A43*, 489−501.
Vidakovic, M., Fraczkiewicz, G., Dave, B. C., Czernuszewicz, R. S., & Germanas, J. (1995) *Biochemistry 34*, 13906−13913.
Vieira, B. J., Colvert, K. K., & Davis, D. J. (1986) *Biochim. Biophys. Acta 851*, 109−122.
Walker, M. C., Pueyo, J. J., Navarro, J. A., Gomez-Moreno, C., & Tollin, G. (1991) *Arch. Biochem. Biophys. 287*, 351−358.
Winkler, J. R., & Gray, H. (1992) *Chem. Rev. 92*, 369−379.
Zanetti, G., Morelli, D., Ronchi, S., Negri, A., Aliverti, A., & Curti, B. (1988) *Biochemistry 27*, 3753−3759.
Zhou, Z., & Swenson, R. P. (1995) *Biochemistry 34*, 3183−3192.
Zhou, Z., & Swenson, R. P. (1996) *Biochemistry 35*, 15980−15988.

BI9709001